APPLICATION OF MARKOV CHAIN MODEL IN STREAMFLOW FORECASTING

A thesis

submitted in partial fulfilment

of the requirements for the degree

of

Master of Science in Geography

at

Massey University

by

Freddie Simon MPELASOKA

MASSEY
UNIVERSITY

1996

Abstract

This thesis presents an approach to streamflow forecasting based on a Markov chain model to estimate conditioned probabilities that a one time-step ahead streamflow forecast will be within a certain streamflow range. In this application a set of "states of flow" defined over streamflow ranges (intervals) forms a finite state space of a Markov chain. Flood forecasting is made by focusing on a preselected state of flow as a flood state.

A multi-objective (two criteria) function for the quantification of the model performance is introduced. Specifically designed for a flood forecasting and warning system the two criteria are the probability of issuing a false alarm and the probability of failing to forecast a flood event. The goal is to minimize both criteria simultaneously together with a preference of accepting more false alarms than misses.

The model has two options of making a forecast: (1) a Threshold Forecast (ThF) approach in which a forecast is based on the probability of making a one-step transition from any state into the flood state; (2) the Most Probable Event (MPE) forecast approach selects the state of flow where the next streamflow is most likely to occur.

Forecasts being probabilistic, there are several options for deciding on when it is appropriate to issue a flood warning in the probabilistic framework. A search for the appropriate probability p_0 is made on interval [0,1] through evaluation of the objective function at each p_0, using data sets from three North Island catchments (Akitio River, Makakahi River and Kiwitea Stream).

The model applying the option of threshold forecasts performed generally well depending on the relative costs assigned to false alarms and misses. The model performed better on the Akitio River which has strongly fluctuating streamflows than on the Makakahi River and Kiwitea Stream which have relatively modest variations in flows.

When the Model applied the option of the most probable event forecasts did not perform well as the probabilities of false alarms were found to be too high for the model to be accepted.

The outcome of this study suggests a simple short-term flood forecasting procedure especially for rivers with strongly fluctuating flows.

Acknowledgements

I would like to use this opportunity to extend my sincere gratitude to all people who assisted me in various ways during all stages of my work. I am grateful to the Government of New Zealand, for a "Spouse's scholarship" extended from the NZODA fellowship which was granted to my wife. Sincere thanks to the Director General, Directorate of Meteorology, Tanzania, for his approval of the offer and travel arrangements to New Zealand.

Special thanks to Mr. Richard G. Heerdegen (Senior Lecturer) for his kind supervision, support and encouragement which facilitated the completion of this work.

I extend my thanks to Dr. Hugo Verela-Alvarez and other staff members of the Massey Computer Services for the consultation time they offered me. Their guidance has been very valuable in my work. I also thank Ms. Marianne Watson, a Resource Data Analyst, Manawatu-Wanganui Regional Council, who played an important role in data acquisition.

I am indebted to my wife Bussakorn, first, for efforts she made to secure the scholarship. Secondly, she had to tighten her schedule of study, so that both of us could study while taking care of our daughter Amy.

This thesis is dedicated to Amy, who at last has Dad and Mum to her self again.

Table of Contents

List of Tables

List of Figures

Chapter 1

INTRODUCTION

Streamflow forecasting is an important component in a variety of routine water management activities. The forecasting problem deals with the development of models which can foretell the future state of streamflow. Its application in this study, however, is aimed at flows associated only with flooding. Flood forecasting is one of the most practicable options in attempts to minimize effects of floods.

1.1 **Rationale of the study**

Like many places in the world, much of New Zealand's developed land, both urban and agricultural, lies in river basins susceptible to flooding. The interaction between the physical flood event and human use of the floodplain results in flood hazard. The level of loss depends on both the characteristics of the flood and the affected human use systems such as the magnitude of the flood and its speed of onset, and the types of land use affected.

Property damage associated with floods ranges from physical destruction of structures caused by water flow to damage due to wetting. Losses from floods can be grouped into three somewhat overlapping types: property damage, social disruption and human casualties.

Any physical material adversely affected by flood water is a property loss, e.g. transport infrastructure, buildings and industrial machinery. In rural areas damage includes loss of stock and crops as a result of siltation and/ or inundation.

Social disruption losses range form re-scheduling to termination of activities in preparation for, and/or as a result of flooding. For example, a damaged factory may

cease production, a damaged transport system will frustrate the distribution of goods and services to and from the community, or disease may breakout due to unsafe water.

While in most cases injuries and loss of lives are minimal, the toll of human suffering and mental anguish as a result of property losses and social dislocation may be very considerable. For example a very disruptive and long term displacement of many families in the Invercargill flood created so much stress that in some cases family breakup took place (Ericksen, 1986).

In general, losses by flood events can really be significant. For the small community of only 3702 people in Paeroa, property loss during the 1981 floods exceeded $7 million and social disruption was estimated at $4 million. A review of flood losses in New Zealand (Ericksen, 1986) suggests that since 1968 the overall flood-loss bill to the nation may be as high as $1.5 billion or $90 million per year, and the losses are continuing to rise.

In order to alleviate the effects of flooding there are several options available, classified into the following three groups:-

(1). Modifying flood events through catchment treatment and river control works. Measures of this type aim to adjust floods to the convenience of people and this may be accomplished in two ways: to alter runoff through catchment treatment measures, and to alter stream flows by use of flood protection structures. Both seek to change parts of the local hydrologic cycle and so reduce the incidence of flooding.

(2). Modification of flood-loss susceptibility through land use management, flood warning, and community preparedness. This approach seeks to alter human use and occupance on floodplains to forms that are more compatible with the flood risk. This may be accomplished through land use management, flood-proofing buildings, emergency programmes or flood forecasting and warning. No attempt is made to modify the magnitude of the flood; rather to lessen flood losses.

Land use management seeks to guide the type of land uses and level of development within flood-prone areas to keep the flood hazard minimal, yet to maximize net benefits from its continued use (Ericksen, 1986). Specific structural design measures that make normal buildings less susceptible to flooding are the usual flood-proofing measures. For emergency procedures, a set of interrelated measures beginning with a flood forecasting and warning system through to individual and collective emergency actions is used to reduce flood-loss susceptibility. Flood forecasting, which provides information on flood levels, is also important for other adjustments, like flood-proofing to work satisfactorily.

(3) Modification of the flood-loss burden is intended to enable affected individuals to share the burden of loss with others, particularly in the unaffected areas. This may be done through pre-event insurance where the individuals pay a premium against losses from flooding they might experience. In effect, the insurance spreads the burden of loss in time and space among insurees. Another approach of burden sharing are the various post-event means which include government grants, subsidies, loans, public appeals for material or funds to help in the relief of flood victims and for rehabilitating affected areas.

The focus in this study is on the flood forecasting and warning option. At a macroeconomic level, the damage that potentially can be prevented by action taken in response to flood forecasts is much greater than the cost of providing forecasts (Krzysztofowicz R. and Davis D. R., 1983). Development of a flood forecasting option as a one of the measures used to mitigate damage from flooding, remains an important area of study in hydrology.

In New Zealand, regional councils are responsible, following the Resource management Act of 1991 for operating flood forecasting systems and for day-to-day monitoring of river flows. Most forecasting methods are classified as "manual", in that they depend on a substantial amount of judgement on the part of the forecaster. The assessments of conditions which could result in flooding are based on the forecaster's previous experience and local knowledge. Rainfall-runoff models and flow-to-flow routing models

are being applied for only a few rivers (Pearson C.P. and Jordan R.S., 1991).

1.2 Criteria for acceptable model forecasts

The best possible forecast is that which completely and identically describes a process which will occur in future. This is, however, difficult to attain since all forecasting techniques contain an element of uncertainty. The acceptable model forecast, therefore, should at least be with minimum variance of forecast errors and it becomes necessary to specify the form and accuracy of the forecast.

In this study a stochastic approach employing a simplified "Markov-chain flow model" is applied to three catchments. The methodology is built around (1) a "Markov-chain flow model" and (2) a model performance quantification objective function. The first element provides a mechanism of short-term streamflow forecasting by estimating the probabilities that the one-step ahead streamflow forecast will be within specified flow ranges. With this approach, flood forecasting is possible by focusing on a pre-selected state of streamflows. The second element establishes the model performance measures and expresses them in terms of a two-criteria objective function to assess the ability of the model to forecast whether the flood threshold probability will be exceeded. The criteria are the probabilities of issuing false alarms and misses prior to flood events. With a desire to simultaneously minimize false alarms and misses, the quantification is designed to serve as a decision aid to the targeted users such as New Zealand regional councils.

The model was tested on the Akitio River, Makakahi River and Kiwitea Stream, all under the jurisdiction of the Manawatu Wanganui Regional Council (North Island). The results aim to provide relevant information on the suitability of the model depending on the costs associated with false alarms and misses of flood events.

Chapter 2

LITERATURE REVIEW

The requirements imposed on forecasting procedures are quite diverse, both in terms of the time scales involved and the type of information desired (Smith, 1991). There are three types of streamflow forecasts: short range (1 hour to 2 days), medium range (2 to 10 days) and long range (more than ten days), depending on the application (Yapo et al., 1993). For example, real time flood warning systems are based on short range forecasts, while hydropower generation operations use medium range forecasts. Irrigation scheduling (Ramirez and Bras [1985]) and municipal domestic water supply operations (Smith [1989], Lettenmaier and Wood [1990]) use long range forecasts.

Generally, there are two approaches to hydrologic modelling: deterministic and stochastic. Stochastic models reproduce the random nature of the relationships between hydrologic inputs and outputs. By contrast, the deterministic approach considers the impact of the physical, chemical and biological processes among the different components of the hydrologic system. Within the system, a limited number of variables are uniquely related by functional expressions or experimental curves to represent a hydrologic system (Yevjevich, 1972). For example this, approach is used in conceptual models such as the Soil Moisture Accounting Model by Burnash (cited by Yapo et al.[1993]).

Natural hydrologic processes are either stochastic or a combination of deterministic and stochastic processes. Deterministic models can describe the reality of a hydrologic system reasonably well, especially in situations when the magnitude of uncertainty is relatively small or negligible. Due to the increasing awareness that there are numerous sources of uncertainty in almost all aspects of environmental modelling, there is need to develop modelling techniques which treat environmental processes as stochastic processes (Zielinski, 1991).

The most frequently used stochastic models are the time series models, used either for hydrologic forecasting or simulation (Yapo et al., 1993), eg. the Autoregressive Moving Average Model (ARMA), the ARMA-Markov model and the Nearest Neighbour Method (Karlsson and Yakowitz, 1987). Cecconi [1988] subsequently presented a step-ahead state forecasting model. This model predicts the future monthly degree of satisfaction with the state of the water supply system, instead of actual supply. The number of states of satisfaction can be varied in the model and he recommends the most useful number of states to be two. Smith [1991] proposed a nonparametric procedure for producing long-range streamflow forecasts. This procedure is based solely on daily streamflow data, utilizing nonparametric regression to relate a forecast variable to a covariate variable.

The Markov process has a voluminous literature encompassing theory and application. Markov chains have been applied to the generation of streamflows for short, medium and long range hydrologic forecasts. The Markov chains approach to rainfall and run-off modelling is not new. In 1957 Gabriel proposed a Markov chain of order one to simulate the occurrence of wet and dry days (Yapo et al.,1993).

Jackson [1975a] used a Markov mixture model to generate synthetic annual streamflows. The model consisted of a two-state Markov chain where the states represented low and normal streamflows, while two normal distributions were used to generate the values of the streamflows in each state.The model was found to be useful for reservoir sizing due to its ability to generate stochastically consistent synthetic streamflow series for long droughts.

Jackson [1975b] also proposed a continuous time Markov chain birth-death process, using discrete streamflow levels as state, to model the phenomenological observation that low streamflow values are more persistent than high streamflow values. The model generated annual streamflows which were used for optimizing reservoir releases.

Haan et al. [1976] presented a first-order Markov chain model and tested it on seven

rainfall stations, using 7 x 7 transition matrices. The class boundaries for the states in the Markov chain were found by using a geometric progression. Simulated rainfall was compared with actual rainfall in several ways, and the model was deemed to perform reasonably satisfactorily.

Yakowitz [1979] proposed a nonparametric Markov model for short-term forecasting. The model consists of inferring the conditional probability distribution of the next streamflow given its recent value. Compared with ARMA models, the nonparametric model was shown to be superior.

Yakowitz [1979] describes the class of N-th order Markov chains as a model for daily stream flow and presents statistical methods for inference within this class. He points out a feature of the N-th order Markov model, which is believed to be unique among streamflow models, that is nonparametric. By this device it is possible to dispense with customary but somewhat dubious assumptions, such as gamma distribution of flows, recessions which are sums of exponentials, and prior assumptions on the distribution of times between extreme events.

Katz [1981] analysed the procedure proposed by Tong in 1975, for estimating the order of a Markov chain based on Akaike's Information Criterion (AIC) and the Bayesian Information Criterions (BIC) proposed by Schwarz [1978]. He concludes that most likely higher than first-order chains need not be considered.

Yakowitz [1985] applied nonparametric modelling of streamflow data to the flood warning problem. In this model, the forecasts are probabilistic and found according to the kernel estimator. He describes a nonparametric inference procedure which converges to the optimal decision function for the flood warning problem as the length of historical record increases for any stationary Markov process by Yakowitz [1985].

Smith et al. [1991] developed a nonparametric framework for constructing distributional forecasts for long-range streamflow variables using conceptual hydrologic models. The

procedure can account for climate information through weighting of historical years and the effects of hydrologic model error. Implementation results suggest that soil moisture information is significantly more valuable than climate information. Climate information is more useful for long-range forecasting of water balance variables, such as accumulated reservoir inflow rather than for base-flow variables such as minimum daily flow.

Yapo et al. [1993] presented a Markov chain flow model for short-term streamflow forecasting in which the forecasts are given as ranges of streamflow values. This model relies on past information such as previous streamflows and precipitation to make forecasts. Three versions were presented: a first order Markov chain model, a second-order Markov chain model and a first-order Markov chain model with rainfall as exogenous input. The model was tested on the Salt River catchment in south-central Arizona, a semi-arid area where the river has erratic streamflows with a coefficient of variation of 2.96. The model performance was good and compared favourably to time series models.

When compared with most stochastic streamflow models, the Markov chain flow model in which data is transformed into ranges of streamflow values, has several advantages over the others. The first advantage is the low vulnerability to calibration data error, due to the fact that exact streamflow values are not needed to determine the transition probabilities. The calculation of transition probabilities only requires knowing the range into which the streamflow value falls.

The second advantage is that the model can use river stage data. Generally, streamflow is not measured directly so measurements of stage are converted to discharge by applying rating curves. The techniques employed to convert stage records to discharge must be carefully calibrated to the gauging site. If the rating curve is not available or of questionable quality, this model can be used to forecast river stage directly (for a stable channel).

For the intended simplified model in this study, Yapo's approach is adopted and only the first-order Markov chain flow model is considered. Two forecast approaches using the model are tested to quantify the model performance through multi-objective function considerations.

The concept of multi-objective function in decision-making has been applied in design, modelling and planning in various fields (Goicoechea at al., 1982). When the formulation of decision-making problem involves a collection of objective functions, two or more of the functions may be similar and in trying to satisfy them simultaneously, the commonly used concept of optimal solution no longer makes sense. Instead of seeking for a single optimal solution, a set of " non-dominated" solutions is sought. The main characteristic of the non-dominated set of solutions is that, for each solution outside this set but still within the feasible region, there is a non-dominated solution for which all objective functions are unchanged or improved and at least one is strictly improved. Given a set of feasible solutions **X**, the set of non-dominated solutions denoted by **S** is defined as:

$$\mathbf{S} = \{x: x \in \mathbf{X}, \text{ there exists no other } x' \in \mathbf{X} \text{ such that } f_q(x') > f_q(x)\}$$
$$\text{for some } q \in \{1, 2, ...p\} \text{ and } f_k(x') \geq f_k(x) \text{ for all } k = q \qquad (1)$$

Thus, it is evident from the definition of **S** that as one moves from one non-dominated solution to another non-dominated solution and one objective function improves, then at least one of the functions must decrease in value.

Chapter 3

MODEL FORMULATION

3.1 Scope

This study focuses on the application of a Markov-chain flow model for short-term streamflow forecasting. Streamflow is expressed in terms of "Markov states of flow" which are defined by streamflow intervals, and are simply called states of flow. The streamflow intervals are determined by clustering analyses explained in sections 3.4.1 and 3.4.2 of this chapter. The model forecasts are presented in terms of states of flow (streamflow intervals). To make forecasts the model employs past records of mean daily streamflows and forecasts are based on the probabilities that the next streamflow will be within a specific state of flow, where the probabilities are conditioned on a one time-step.

Flood event forecasting and warning are used to quantify the model performance. Designed as a statistical decision-making problem for operational purposes, a two criteria objective function is formulated. The criteria are the probabilities of issuing 'false alarms' and 'misses'. In this context a false alarm is an event when a warning is issued and the flood itself does not occur; a miss is an event when an alarm is not issued yet a flood occurs.

For a warning system to be considered reliable, it is important to minimize both false alarms and misses. These two possibilities can be quantified by probability measurements, since the probability of a false alarm and the probability of a miss are measures of the likelihood of these two events taking place.

3.2 Concept

The process of streamflow is assumed to be a phenomenon that varies as time advances, and that the variation has a significant chance component in it i.e. a stochastic process. It is further assumed that the process satisfies the property of a Markov chain. A Markov chain is a stochastic process having the property such that the value of the process X_t at time *t*, depends only on its value at time *t-1*, X_{t-1}, and not on the sequence of values X_{t-2}, X_{t-3}, ..., X_0 that the process passed through in arriving at X_{t-1}. Thus no matter what the past was, the current state of the flow is all that is needed to predict the future flow.

A streamflow time series $\{x_t\}$ can be transformed into several states of flow defined over intervals of streamflow values. Streamflow variations being a time-oriented physical process that is controlled by a random mechanism, the transformation results in another sequence of states of flow $\{X_t\}$ where t is a time or sequence index. At a particular time t the process is in exactly one of M mutually exclusive and exhaustive states of flow. The system states of flow can be labelled 1, 2, 3,..... M. The random variables X_1, X_2, ... represent the system states of flow at time 1 day, 2 days and so on from some start date of observations.

The streamflow process is assumed to be time-discrete and the events' statistical independence is relaxed to allow a one-step (stage) dependence. The predictions of the future streamflow state, once the current streamflow state is known, cannot be improved by additional knowledge of the past. The words "additional knowledge" are crucial: there is no implication that the past is devoid of the information about the future, only that once the current state is known, the past contains no further information. Essentially this is due to the fact that the streamflow assumes the property of a Markov chain.

The probability, that the process at time *t+1* will be in 'state' *j* given that at time *t* the process was in 'state' *i*, is given by the conditional probability:

$$p_{ij} = p\{X_{t+1} = j | X_t = i\} \quad (2)$$

Equation 2 is the one-step transition probability. That is, it is the probability that the process makes the transition from state *i* to state *j* in one time period. If the process is divided into M states, then M^2 transition probabilities must be defined. However at each step the process must either remain in state *i* or proceed to one of the other M-1 states.

$$\sum_i p_{ij} = 1 \quad (3)$$

The transition probabilities can be arranged in a matrix known as the Transition Probability Matrix. The Transition Probability Matrix is a M x M stochastic matrix such that $p_{ij} > 0$ and $\sum_i p_{ij} = 1$ for all i, j.

The elements of the Transition Probability Matrix can be estimated by the method of maximum likelihood by taking the ratio n_{ij}/n_i, where n_{ij} represents the number of transitions from system state *i* to *j* in one step and n_i is the number of times the streamflow is in state *i*. The validity of the maximum likelihood estimates of the transition probabilities is shown in Appendix I.

As the Markov chain advances in time the probability of being in state *j* after a large number of steps becomes independent of the initial state of the chain X_0. When this occurs the chain is said to have reached a steady state under which there exists a steady state probability vector **P** such that **P** = **P** x TPM. One can determine **P** by iterative matrix multiplication of the TPM, where TPM is the transition probability matrix.

3.3 Model parameters

A Markov chain flow model is said to be of k^{th} order, if k is the minimum number of terms, prior to X_{t+1} in the streamflow state series $\{X_t\}$, that are sufficient to characterize its probabilistic behaviour. In this application k is equal to 1, hence a one-time step Markov-chain flow model. Other model parameters are defined as follows: M is the number of streamflow states where $X_t \in \{1,2,...,M\}$ for all t and q_i is the upper bound of the i^{th} streamflow range where $q_1 <....< q_{M-1}$.

83.4 Streamflow states and associated flow intervals

The number of streamflow states M and the corresponding streamflow intervals can be selected in a heuristic fashion. In order to eliminate the subjectivity in the choice of intervals, the literature recommends the use of clustering algorithms; statistical software (Minitab, 1994) was used in this analysis.

3.4.1 Cluster of Observations analysis

To determine the number of streamflow states of the Markov chain under study clustering of observations is carried out. This analysis performs agglomerative hierarchical clustering of observations. Essentially, the clustering of observations is to help classify observations into groups, where the groups are initially unknown. The operation begins with all observations separate, each forming its own cluster. In the first step the two observations closest together are joined. In the next step, either a third observation joins the first two, or two other observations join together to form a different cluster. Each step results in one less cluster than the step before until, in the end, all cases are combined in one cluster.

The program decides which clusters are closest together depending on distance definition and the link method. Final partition is the grouping of clusters which will identify

groups whose members share common characteristics. The similarity and distance level values are listed under "Amalgamation Steps". The changes in the pattern of similarity and/or distance levels help in choosing the final groupings.

3.4.2 Cluster K-means analysis

In order to establish the intervals of the streamflows associated with each state, K-means analysis is used. This analysis assigns observations into a pre-determined number of groups. This number of groups is determined by the cluster of observations as outlined in section 3.4.1. The program evaluates each observation, moving it into a group whose centroid it is closest to, using "Euclidean distance" (defined in Appendix II). When a group changes, by losing or gaining an observation, the program recalculates the group centroid. This process is repeated until no more observations can move into a different group, i.e. until all observations are in the group to whose centroid they are closest. At this point the range of observations in a group forms the streamflow interval which defines a state of flow.

To a set of streamflow intervals with boundaries q_i, the following mapping is applied to the streamflow time series $\{x_t\}$ to obtain the streamflow range series $\{X_t\}$.

$$\begin{aligned} X_t&=1 \qquad 0 \le x_t \le q_1 \\ X_t&=i \qquad q_{i-1} < x_t \le q_i, \quad \text{for } i= 2, ..., M - 1 \\ X_t&=M \qquad x_t > q_{M-1} \end{aligned} \tag{4}$$

Then the state of streamflow at any time t is defined by one of the states in the state space {1, 2, ...M} and the transition probabilities from state to state are computed by equation (2).

3.5 Forecasts

For purposes of forecasting floods a streamflow value F is defined such that whenever the streamflow x_t is greater than F, a flood is deemed to occur. Thus F is the threshold streamflow level for a flood. In terms of streamflow ranges, x_t belongs to the streamflow range (F,+infinity) which is equivalent to $X_t = M$; the M^{th} streamflow state is the flood state and $q_{M-1} = F$; (equation 4).

To quantify the performance of the model in flood prediction, two types of forecasts are investigated in the application of this model: threshold and most probable event forecasts.

3.5.1 Threshold forecasts

From the definition above where the M^{th} streamflow range (F,+infinity) is the flood state, the flood probability forecast can be determined from the last column of the Transition Probability Matrix. The last column of a transition probability matrix represents the probability of making a one-step transition from any state into the flood state. Ideally, it would be safer to issue a flood warning every time the probability of a flood is not zero. However, that is likely to result in many false alarms and may lead to loss of confidence in the reliability of the forecasts. Based on the probability of the next streamflow being in the flood state a decision must be made as to whether to issue a flood warning or not. It is appropriate to choose to issue a warning only if the flood probability prediction exceeds some threshold value. This is where a study of the trade-off between false alarms and misses becomes necessary. Bearing in mind that the 'cost' of a miss can be substantial, an attempt is made to determine appropriate threshold probabilities.

3.5.2 The most probable event forecast

The most probable event forecast selects the streamflow range in which the next streamflow is most likely to occur.

$$X_{t+1} = \{j:\max_{j} p_{ij}\} \quad (5)$$

where j represents the state of the streamflow at time t+1. The state i contains information about the current observed streamflow value. The forecast considers all streamflow ranges through the p_{ij} in contrast to the threshold probability forecast.

3.6 The Multi-objective function

To quantify the performance of the Markov flow model in forecasting floods, a two-decision variable objective function is formulated from decision theory consideration. For a flood forecasting situation the decision has to be made to issue a warning or not. Associated with these options is the occurrence or non-occurrence of a flood. Let nHf be the number of correct predictions at flood level, nHnf the number of correct predictions at non-flood level, nMs the number of misses, and nFA the number of false alarms. Since a good model for flood forecasting is one which is able to correctly predict the occurrence of flood events, there is need, therefore, to simultaneously maximize the number of hits at nHf and nHnf. This maximization is equivalent to simultaneously minimizing the number of false alarms nFA and misses nMs. Let a two-criteria function H() = [P(FA),P(MS)], describe the probability of the occurrence of false alarms and misses, where P(FA) and P(Ms) are probabilities of false alarms and misses respectively. P(FA) and P(Ms) can be estimated by equations 6 and 7 when the threshold probability p_0 is varied on the interval [0,1].

$$P(FA) = \frac{nFA}{nHnf+nFA} \quad (6)$$

$$P(Ms) = \frac{nMs}{nHf+nMs}$$

The function is explicitly used to minimize both the likelihood of issuing false alarms and the likelihood of failing to issue warnings prior to flooding.

To identify the set of non-dominated solutions, points from the P(FA)P(Ms) decision space are mapped onto the F objective function space, using the objective functions P(FA) and P(Ms) estimates (equation 6 and 7). The pair [P(FA),P(Ms)] at some p_0 in [0,1] represents a point in the P(FA)P(Ms) plane. By definition the obtained points are examined for non-dominated solutions.

For simplicity, however, it is assumed that we are willing to accept more false alarms than misses. Under this preference, the search for the appropriate threshold probability p_0 is associated with the set of non-dominated points (solutions) where P(FA) > P(Ms).

3.7 Catchments under study

Daily mean streamflow data from three catchments were used for calibration, verification and model performance quantification. Catchments' descriptions are given in the following sections and their locations are shown on the map (Appendix V).

3.7.1 Akitio catchment

The Akitio River rises on the eastern side of the North Island of New Zealand and drains south-eastward into the Pacific Ocean. The drainage basin is elliptical and aligned in a general NNE to SSW direction following the orientation of the ranges. Catchment altitude ranges from sea level to 800m. The eastern slopes of the Puketoi Range are a fault scarp and are therefore very steep.

The upstream area is comprised of siltstone, sandstones and calcareous mudstone. The central areas of the catchment are made up of calcareous sandy siltstone. A significant area of the coastal part of the catchment is comprised of silts and conglomerates. The area north and east of the Puketoi Range is heavily faulted giving rise to a rather complex drainage network.

The catchment has been cleared of native bush cover except for small areas along the river margins north of Weber and pockets along the ridge of the Puketoi Range. Approximately one third of the catchment above the flow measuring station is poor pasture and scrub with pastoral farming as the predominant land use. The township of Akitio, on the coast, supports some fishing and recreational activities.

The climate is influenced by the location of the Tararua Ranges and the predominant westerly winds over New Zealand. The ranges shelter the northern part of the catchment from the westerly winds and consequently rather high temperatures with dry weather can be experienced. The north-westerlies over the Manawatu Gorge enhances cloud cover and rainfall on the Puketoi Range because of its orographic effect while east of the Range it becomes very dry if the north-westerlies prevail for extended periods. The weather systems from the south and the east, particularly decaying storms of tropical origin passing east of New Zealand, are important rain bearing systems. Due to the coastal hills, rapid orographic uplift of the moist air can result in very heavy rainfalls. Rainfall in the southern part of the catchment under the influence of the coast hills is about 1100mm per year. The central area of the catchment receives less than 1000mm in an average year while in the neighbourhood of the Puketoi Range annual rainfall exceeds 1600mm per year.

The Akitio River flow is derived primarily from rainfall derived runoff with very little sustained base flow. The combination of lithology and climate results in large flow variations and the difference between low flows and flood flows is very large. Catchment yield ranges from 0.1 l/s/km^2 to 3600 l/s/km^2 or more. The catchment responds relatively slowly to rainfall although several flood events occur every year. The

duration of a flood event may extend to more than five days although peak flows are rarely sustained for more than a few hours. There is no runoff from snowmelt and there are no significant permanent ponding areas such as reservoirs or lakes.

Very little water is used for out-of-stream purposes as so little water is available for a large portion of the year.

3.7.2 Makakahi catchment

The Makakahi River rises on the south-eastern slopes of the Tararua Ranges. These ranges form the southern portion of the main axial divide of the North Island. The river flows in a north-east direction to join two larger rivers, the Mangatainoka and Tiraumea before flowing into the Manawatu River upstream of the Manawatu Gorge. The Manawatu River flows via the Gorge, from one side of the axial ranges to the other and subsequently south-west to the coast into the Tasman Sea. The Makakahi catchment altitude ranges from 190m to 980m with the upper portion being very steep. The drainage basin is long and narrow and aligned with the Range.

The eastern part of the catchment is predominantly fossiliferous calcareous sandy siltstone. The western part is made up of fluvial deposits, derived in the main from former river channels. The northern part is composed primarily of argillite and greywacke. Pastoral farming is the predominant land use, with less than one percent of the catchment area under bush cover.

The climate is dominated by the orographic effects of the Tararua Ranges and the predominant westerly winds over the country. The catchment also experiences weather associated with systems from the south and east which enhance rainfall through orographic effect. Rainfall varies from 4000mm per year on the tops to less than 1200mm per year in low areas. Although it rains throughout the year highest rainfall is in winter.

The flow in the Makakahi River is derived primarily from rainfall with base flow from water stored in large fluvial deposits. Catchment yield ranges from 1 l/s/km^2 to 1300 l/s/km^2 or more. The catchment responds rapidly to rainfall and may experience several flood events in a year. Flood event duration rarely exceeds 48 hours.

3.7.3 Kiwitea catchment

The Kiwitea Stream rises in rolling to steep hilly land to the west of the western slopes of the Ruahine Ranges. The stream flows in a SSW direction to join a large river, the Oroua, before flowing into the Manawatu River. Catchment altitude ranges from 90m to 650m with the lower part being quite flat in contour. The drainage basin is long and narrow and aligned with the Range.

The headwaters are predominantly marine fossiliferous sands and gravels with some limestone horizons. The central areas of the catchment are made up of basal conglomerates and marine sands which lead to undifferentiated alluviums in the lower areas of catchment.

Forty percent of the catchment is developed into high producing pasture, with dairying a prominent activity. There is increasing use of land for horticulture and cropping, particularly fodder crops and potatoes. To a lesser extent intensive grazing occupies the undulating central areas. The indigenous forests have been cleared.

The orographic effects of the Ruahine Ranges on the predominant westerly winds influence the weather. Rainfall in the lower catchment is about 850mm per year (a rather dry area for the North Island), while higher areas receive up to 1600mm in an average year. Even though its rainfall is evenly distributed over the year, there is a slight winter maximum.

Flows in the Kiwitea are primarily from rainfall. Catchment yields range from 0.5 l/s/km^2 to 700 l/s/km^2. The catchment responds rapidly to rainfall and floods can be

experienced.

Extensive use of water out-of-stream is made for agricultural purposes, particularly for pasture and for the irrigation of crops.

Table 3.1 Summary of River / Stream Statistics

River/Stream	Station		Period		Statistics				Area
	Name	No.	Start Date	End Date	Min. l/s	Max. l/s	Mean l/s	Cv	km^2
Akitio	Weber	25003	02 Nov 1979	27 Jul 1994	12	180983	2427	3.4	123
Kiwitea	Spur R/Ext	1032516	05 Nov 1976	20 Jul 1992	90	165981	5868	1.6	246
Makakahi	Hamua	1032518	19 Dec 1979	05 Aug 1991	45	65705	2041	1.7	158

The data in Table 3.1 consists of mean daily flows for the Akitio River at Weber (15 years), the Makakahi River at Hamua (16 years), the Kiwitea Stream at Spur Road Extension (12 years). With a coefficient of variation of 3.4, streamflow in the Akitio River is very erratic. The Akitio has registered a minimum of flow of 12 l/s compared with 90 l/s for the Makakahi River and 45 l/s for the Kiwitea stream. The Akitio River has also the largest maximum flow. The three rivers have high flows associated with the winter season.

Chapter 4

MODEL APPLICATION

Details of the three catchments used in this study are given in Chapter 3 and summarized in Tables 4.1 and 4.2.

4.1 Streamflow regimes

The averages of mean monthly streamflows over the years of record were calculated for each month, January to December, and are given in Tables 4.1. Table 4.2 shows these mean monthly flows for the three catchments converted into specific discharges. During the winter months (June - September) the flows as shown in Table 4.4 are generally consistent with coefficient of variation (Cv) less than 1.3 and the highest flows occurring in July. On the contrary, relatively low and erratic flows with Cv greater than 2.9 occur during summer months (December - March).

The runoff variations described by histograms in Figures 4.1, 4.2 and Figure 4.3 exhibit distinctive seasonal patterns which are referred to as "regimes". Despite the differences in their respective flow magnitudes, the histograms show regime similarity for the three catchments. All of these catchments have a single period of high flows followed by a single period of relatively low flows. Although general similarities can be pointed out between these regimes on the basis of monthly mean flows, streamflow variations based on daily or shorter-period data are likely to vary considerably and indeed at this level of detail each river/ stream may behave uniquely. The hydrographs of daily mean discharge shown in Figures 4.4, 4.5, 4.6, 4.7, 4.8 and Figure 4.9 must be regarded, therefore, simply as examples selected to illustrate broad contrasts in catchment hydrology rather than as formal representation of identifiable categories of flow variation.

Monthly specific discharge histograms for the Akitio River are shown in Figure 4.1. Large differences between low flows and high flows suggest the strongly fluctuating dischages by the Akitio River. Catchment yield ranges from 2 - 45 l/s/km^2. The Makakahi River flow, (Figure 4.2) on the other hand, shows a gradual and moderate flow, variations. The large differences between low and high discharges in the monthly specific discharges for Kiwitea Stream in Figure 4.3 indicate the lowest catchment yield to be about 2 l/s/km^2 and the biggest yield to be 18 l/s/km^2.

Table 4.1 Mean monthly streamflows

River	Flow (l/sec)											
	Jan	Feb	Mar	Apr	May	Jun	Jul	Aug	Sep	Oct	Nov	Dec
Akitio	318	1146	1599	1956	20586	4222	5496	3765	4198	2131	1270	1104
Makakahi	2704	2788	3336	4313	776	8101	9601	8541	8570	6944	4152	4826
Kiwitea	636	475	936	1221	1900	2874	4259	3933	3446	2829	1317	845

Table 4.1 shows the average monthly flows. It can be noted that winter flows predominate in all cases and are almost double the summer flows.

Table 4.2 Mean monthly specific discharge

River	Discharge (l/sec/km^2)											
	Jan	Feb	Mar	Apr	May	Jun	Jul	Aug	Sep	Oct	Nov	Dec
Akitio	2.6	9.2	13.0	15.9	16.7	34.3	44.7	30.6	34.1	17.3	10.3	9.0
Makakahi	17.1	17.6	21.1	27.3	42.9	51.3	60.8	54.1	54.2	44.0	26.3	30.5
Kiwitea	2.6	1.9	3.8	5.0	7.7	11.7	17.3	16.0	14.0	11.5	5.4	3.4

From Table 4.2 the Kiwitea Stream appears to have much lower specific discharges than the other two rivers.

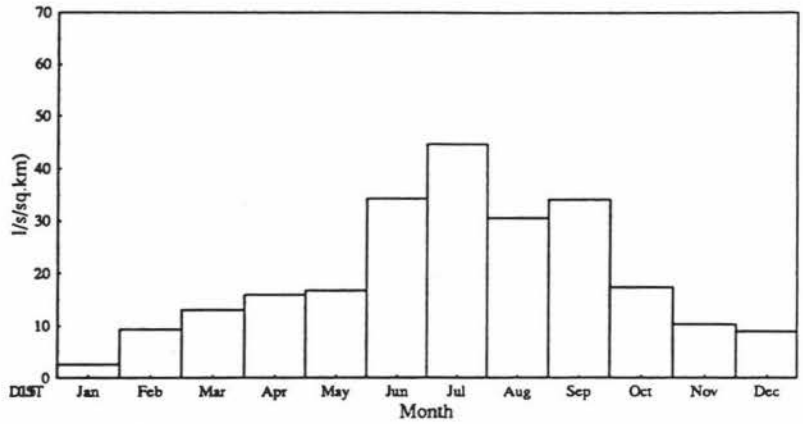

Fig. 4.1 Monthly specific discharge. Akitio River.

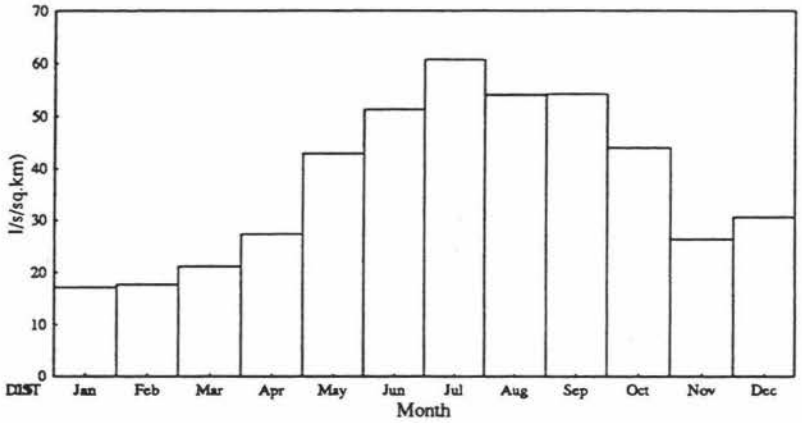

Fig. 4.2 Monthly specific discharge. Makakahi River.

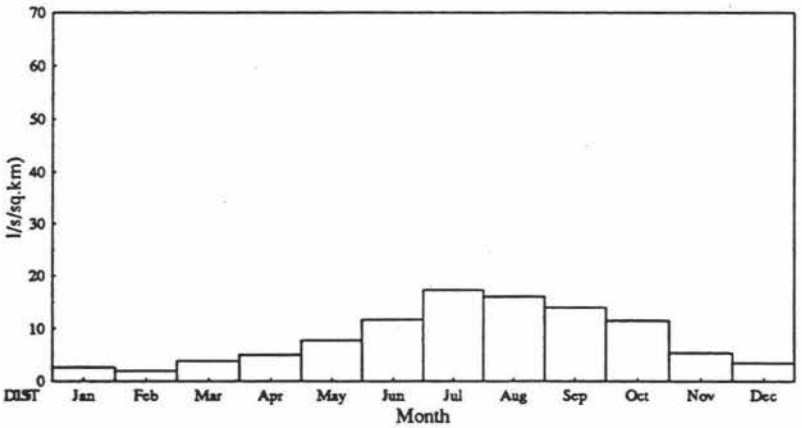

Fig. 4.3 Monthly specific discharge. Kiwitea Stream.

4.2 Seasonal data sets

Due to annual cyclicity brought about by seasonal change, the catchments' response stationarity is approximated by restricting attention to flows during more stable portions of the year, namely winter and summer periods. Therefore for each catchment two data sets were considered and each set was partitioned into model calibration and verification data as shown in Table 4.3. The winter data sets covered the periods 1st June - 30th September and 1st December to 31st March for summer.

Table 4.3 Calibration and Verification data sets

River / Stream	Calibration period	Verification period
Akitio	1980 - 1991	1992 - 1993
Makakahi	1980 - 1988	1989 - 1990
Kiwitea	1976 - 1989	1990 - 1992

The Kiwitea Stream data covered the longest period of record of 17 years followed by the Akitio River, 14 years, and the Makakahi River data was of 11 years. The statistics of the seasonal data sets are given in Table 4.4.

Table 4.4 Statistics of the seasonal data

River / Stream	Period				Statistics							
	Winter		Summer		Winter				Summer			
	S/Date	E/Date	S/Date	E/Date	Min l/s	Max l/s	Mean l/s	Cv	Min l/s	Max l/s	Mean l/s	Cv
Akitio	1980	1993	1979	1993	190	1000000	5600	5.4	12	60311	943	4.0
Makakahi	1980	1990	1980	1990	980	86952	8617	1.2	90	103047	3010	2.2
Kiwitea	1977	1991	1976	1992	272	65705	3431	1.3	46	32485	697	2.4

As Table 4.4 shows, in general the streamflow variability tends to be greatest in summer and least in winter over the three catchments. The Akitio River's flow tends to be erratic in both seasons.

Erratic streamflows in Akitio River can be associated to the heavy flash-rainfalls, a typical characteristic of the eastern catchments of the North Island (Murray D. L. and Ackroyd P.,1979).

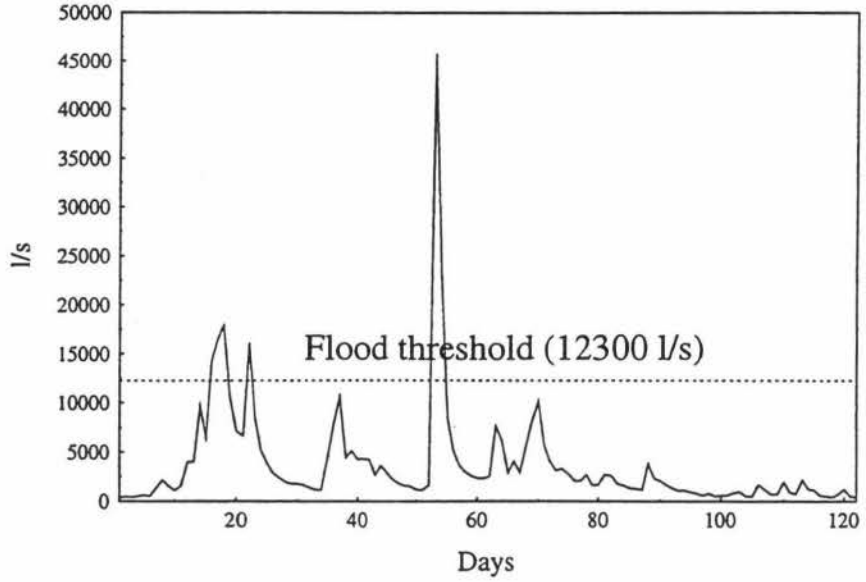

Fig. 4.4 Hydrograph. Akitio River, winter 1980.

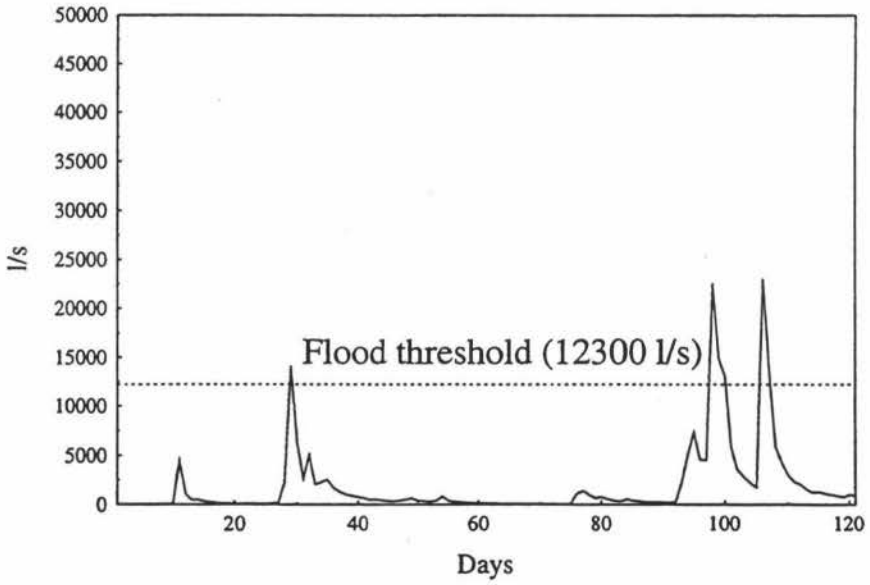

Fig. 4.5 Hydrograph Akitio River, summer 1979/80.

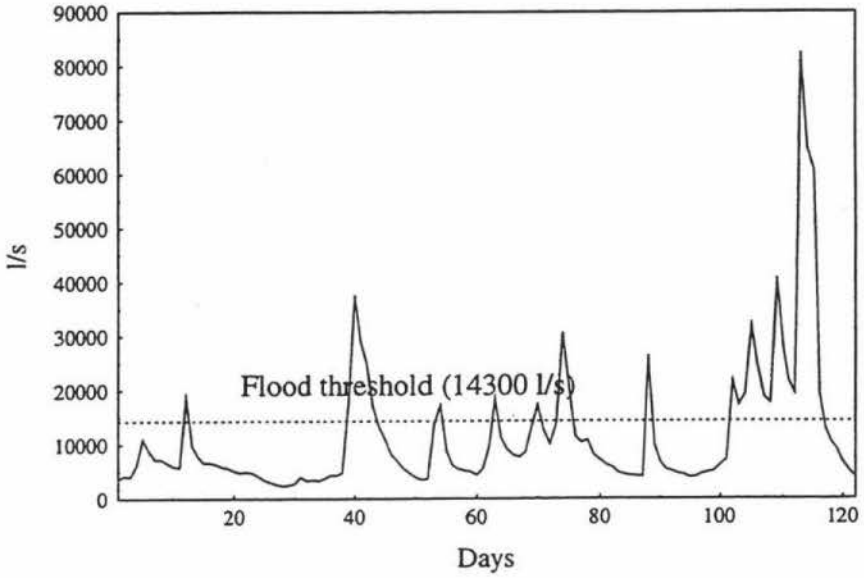

Fig. 4.6 Hydrograph. Makakahi River, winter 1980.

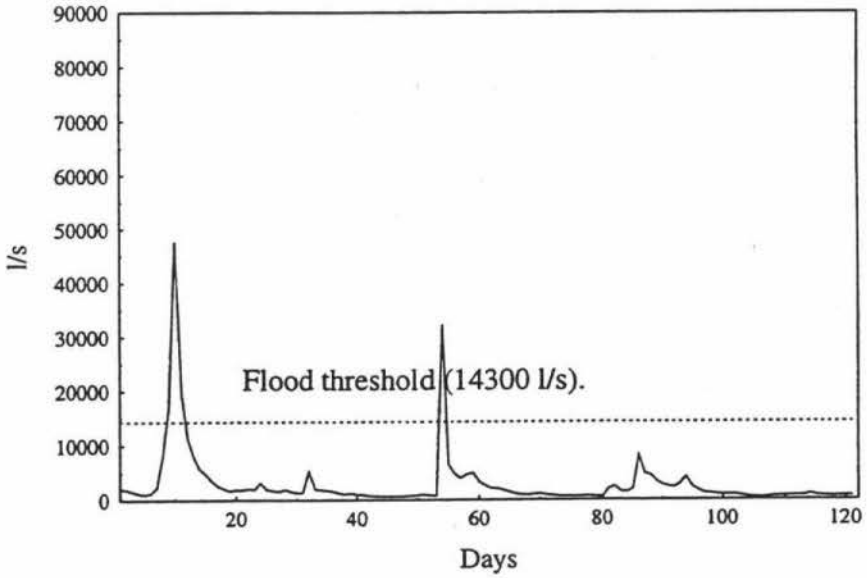

Fig. 4.7 Hydrograph. Makakahi River, summer 1980/81.

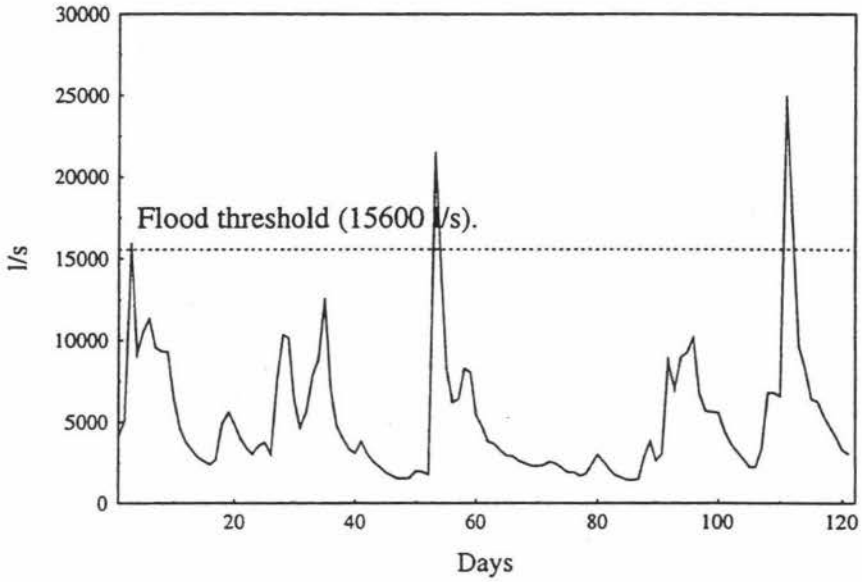

Fig. 4.8 Hydrograph. Kiwitea Stream, winter 1977.

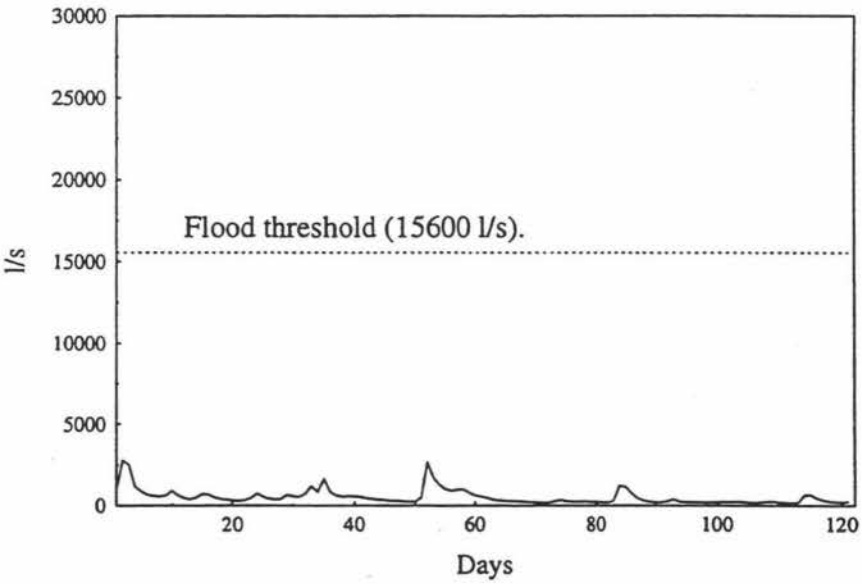

Fig. 4.9 Hydrograph Kiwitea Stream, summer 1976/77.

The Akitio River hydrographs in Figure 4.4 and 4.5 show large flow variations and a large range between low and high streamflows. The river has low streamflows most of the time.

The streamflow in the Makakahi River (Figures 4.6 and 4.7) is sustained by base flow and may experience several floods in a season.

The streamflow of the Kiwitea Stream as shown by the hydrographs in Figures 4.8 and 4.9 depends primarily on direct rainfall runoff and there is no sustained base flow. Summer flows are mostly low flows.

4.3 Results and Discussion

4.3.1 Streamflow transformation into "States of flow"

A reasonable number of streamflow values have to be observed within a range that defines a state of flow (Yapo et al., 1993). Adjustments are made when necessary to make sure a reasonable number of streamflow values are observed within each range. A range (state) has at least $n^{1/3}$ observations where n is the total number of observations. Streamflow ranges are determined by clustering analysis in order to eliminate the subjectivity in the choice of intervals.

Clustering analysis on calibration data sets is made in two steps. The first step is the "Clustering of Observations" analysis which is carried out on the calibration data sets for winter and summer seasons for the Akitio River, Makakahi River and Kiwitea Stream. The purpose of this analysis is to determine the desired number of streamflow groups (clusters) of observations. The analysis revealed an acceptable number of streamflow groups for each data set.

Clustering of Observations analysis is followed by the "Cluster K-means" analysis which

assigns the observations to the streamflow groups until all observations are in the streamflow groups to whose centroid they are closest. The acceptable streamflow intervals which define the states of flow during winter and summer months for the three rivers were established, and are discussed in the following sections.

4.3.1.1 Akitio River at Weber

The flows of the Akitio River at Weber are classified into 6 streamflow states during winter and 7 states during summer as shown in Tables 4.5 and 4.6. Streamflow state 6 is the flood state at Weber during winter with a mean flow of 42936 l/s while in summer a flood streamflow state is 7 with a mean flow of 34318 l/s. Winters experience 9 times more floods than summers.

During winter low streamflows (states 1 and 2) constitute 75% of the total number of observations (days), while the flood states constitute 7%. During summer, low flows constitute 91% of the total number of observations, and only 0.8% are flood states.

Table 4.5 Winter streamflow states. Akitio River.

State (St_i)	Flow interval l/sec	Freq.	Mean flow l/sec	Cum. Freq.	% Cum. Freq.
6	12227 - infinity	102	42936	102	7
5	7480 - 12226	94	9424	196	13
4	4270 - 7479	119	5825	315	22
3	4262 - 4761	48	4494	363	25
2	3212 - 4261	121	3693	484	33
1	0 - 3211	979	1461	1463	100

Table 4.6 Summer streamflow states. Akitio River.

State (St_i)	Flow interval l/sec	Freq.	Mean flow l/sec	C/Freq.	% C/Freq.
7	17801 - infinity	11	34318	11	0.8
6	9806 - 17800	16	14572	27	1.9
5	4850 - 9805	25	6873	52	3.6
4	2804 - 4849	34	3827	86	5.9
3	1639 - 2805	46	2196	132	9.1
2	624 - 1638	161	1009	293	20.2
1	0 - 623	1159	166	1452	100.0

The frequencies of occurrence of streamflow states are listed in Tables 4.5 and Table 4.6 starting from the highest to the lowest streamflow state. Cumulative frequencies were converted into percentages of the total number of days and plotted to give a flow-duration curve that gives the percentage of time during which any selected state of streamflow could be equalled or exceeded. Figures 4.10 and 4.11 show the flow-duration curves during winter and summer seasons respectively. The curves are plots of percentages of cumulative frequencies of streamflow states rather than the cumulative frequencies of streamflow values. Although these are not true flow duration curves, it should be noted that the summer curve has fewer high flow states than in winter which is entirely consistent with conditions on the East Coast.

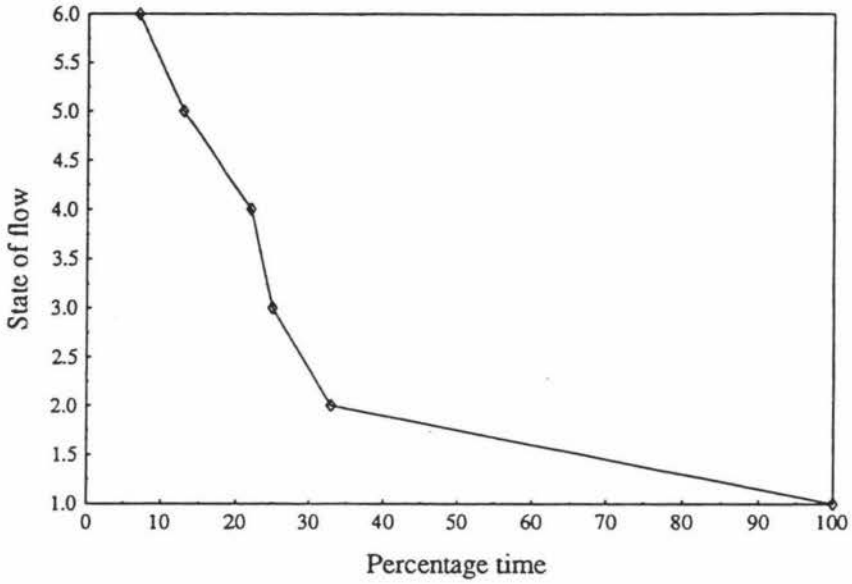

Fig. 4.10 Winter Flow Duration curve. Akitio River.

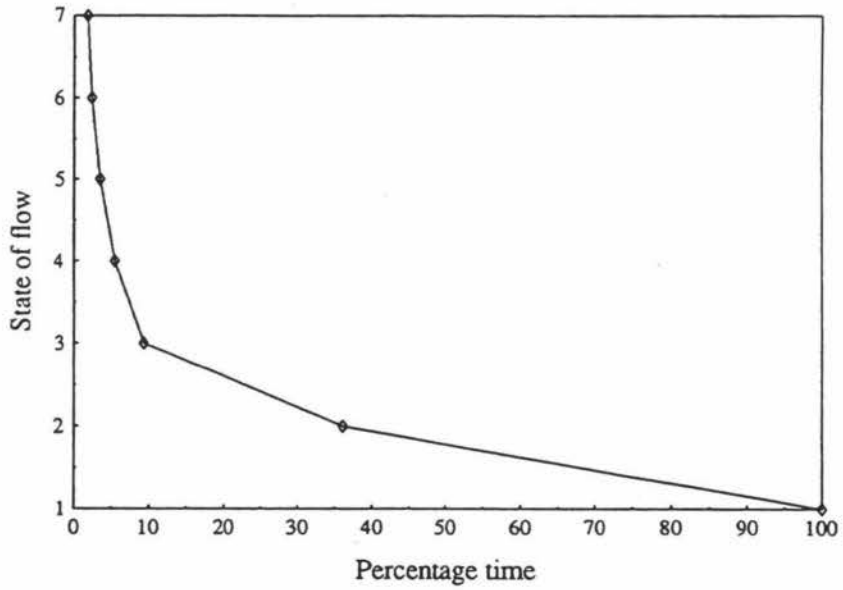

Fig. 4.11 Summer Flow Duration curve. Akitio River.

4.3.1.2 **Makakahi River at Hamua**

The state of flow of the Makakahi River at Hamua, is categorized into 6 states of flow during both winter and summer months as shown in Tables 4.7 and 4.8 Streamflow state 6 is the flood state at Hamua during winter with a mean flow of 27674 l/s. The summer flood state is also 6 with a mean streamflow of 29545 l/s. On average, winter months experience 5 times more floods than summer months and in general summers have lower volumes of streamflow.

During winter, low streamflows (states 1 and 2) constitute 73% the of total number of observations and flood states constitute 14%. During summer, low flows constitute 85% of the total number of observations and 3% are flood states.

Table 4.7 Winter streamflow states. Makakahi River.

State (St_i)	Flow Interval l/s	mean flow l/s	freq.	Cum freq.	% cum freq.
6	14500 - +++	27674	176	176	14.4
5	12619 - 14499	13370	36	212	17.4
4	10992 - 12618	11848	49	261	21.4
3	9154 - 10991	10127	68	329	27.0
2	5378 - 9153	6949	263	592	48.5
1	0 - 5377	3286	628	1220	100.0

Table 4.8 Summer streamflow states. Makakahi River.

State (St_i)	Flow Interval l/s	mean flow l/s	freq.	Cum freq.	% cum freq.
6	14301 - +++	29545	36	36	3.3
5	10764 - 14300	12131	21	57	5.2
4	7193 - 10764	8675	37	94	8.6
3	4850 - 7192	5880	71	165	15.2
2	2126 - 4849	3210	187	352	32.3
1	0 - 2125	842	737	1089	100.0

The frequencies of occurrence of streamflow states are listed in Tables 4.7 and 4.8 starting from the highest to the lowest streamflow state. Cumulative frequencies were converted into percentages of the total number of days and plotted to give a flow-duration curve that gives the percentage of time during which any selected state of streamflow could be equalled or exceeded. Figures 4.12 and 4.13 show the flow-duration curves during winter and summer seasons respectively. The two curves are more or less the same (similar slopes) except the area under the curve is bigger in winter which indicates that larger volumes of flow are in winter.

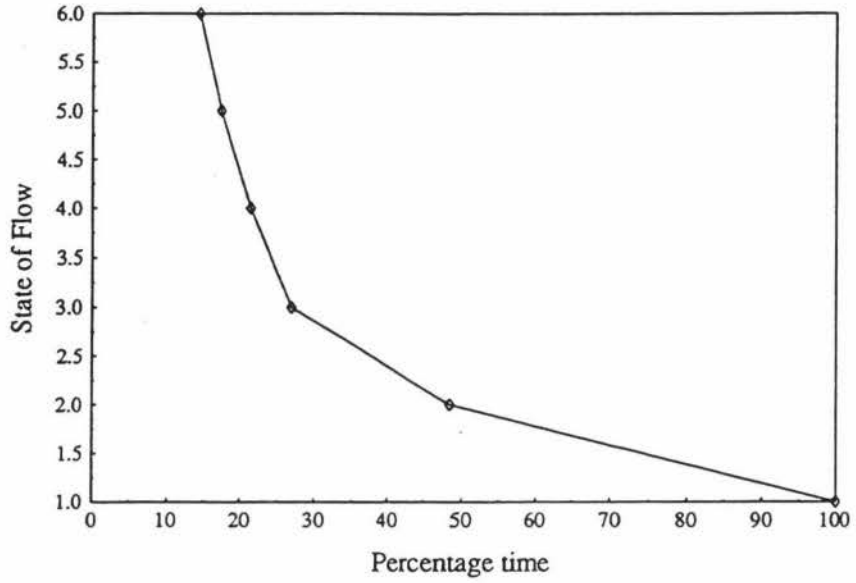

Fig. 4.12 Winter Flow Duration curve. Makakahi River.

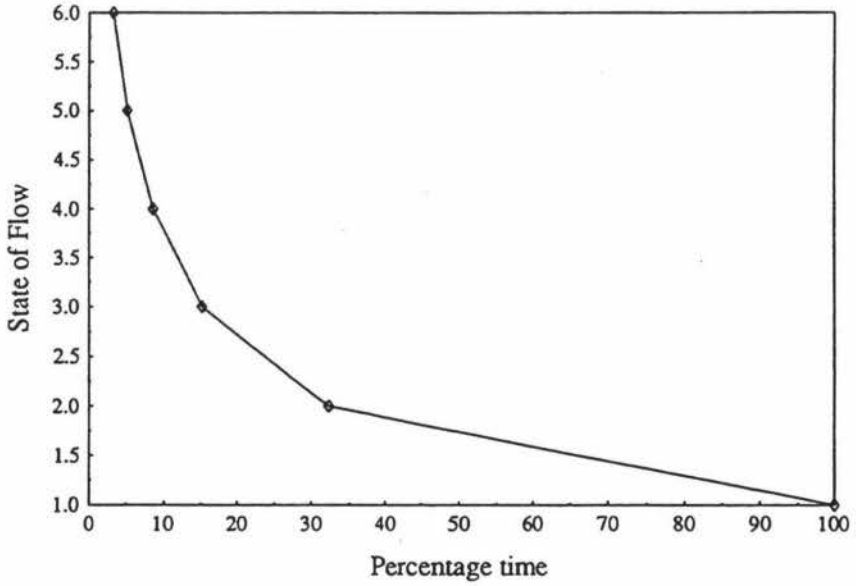

Fig. 4.13 Summer Flow Duration curve. Makakahi River.

4.3.1.3 Kiwitea Stream at Spur Rd. Extension

The streamflow of Kiwitea Stream at Spur Rd. Extn., is categorized into 7 states of flow during winter and 5states of flow as shown in Tables 4.9 and 4.10. During winter, the flood state has a mean flow of 27860 l/s. Low streamflows (states 1 and 2) constitute 70% of total number of days, and flood states constitute 2%. In summers the streamflows are low and the highest state has a mean flow of 10371 l/s. Due to the fact that no high flows seem to have been experienced during summer the flood flows are not considered in this case.

Table 4.9 Winter streamflow states. Kiwitea Stream.

State	Interval l/s	Mean flow l/s	Freq.	Cum. Freq.	% Cum.Freq.
7	155501 - ++	27860	29	29	1.8
6	15550 - 15549	12373	43	72	4.5
5	6800 - 10549	8404	117	189	11.9
4	4817 - 7699	5711	122	311	19.6
3	3394 - 4816	3992	181	492	31.0
2	1567 - 3393	2415	463	955	60.2
1	0 - 1566	919	631	1586	100.0

Table 4.10 Summer streamflow states. Kiwitea Stream.

State	Interval l/s	Mean flow l/s	Freq.	Cum. Freq.	% Cum. Freq.
5	4762 - +++	10371	29	29	1.7
4	2214 - 4761	3172	58	87	5.1
3	1011 - 2213	1426	132	219	12.9
2	418 - 1010	637	422	641	37.8
1	0 - 417	226	1053	1694	100.0

The frequencies of occurrence of streamflow states were listed in Tables 4.9 and Table 4.10. Cumulative frequencies converted into percentages of the total number of days were plotted to give a flow-duration curves for both winter and summer months. Figures 4.14 and 4.15 show the flow-duration curves during winter and summer seasons respectively. The summer curve is steeper and less full than the winter curve. It shows that the area under the winter flow-duration curve is bigger than the area under the summer curve, and hence, bigger volumes of streamflow are experienced during winter months. However, the difference between summer and winter is not clearly as marked as in the eastern catchments of the Akitio and Makakahi Rivers.

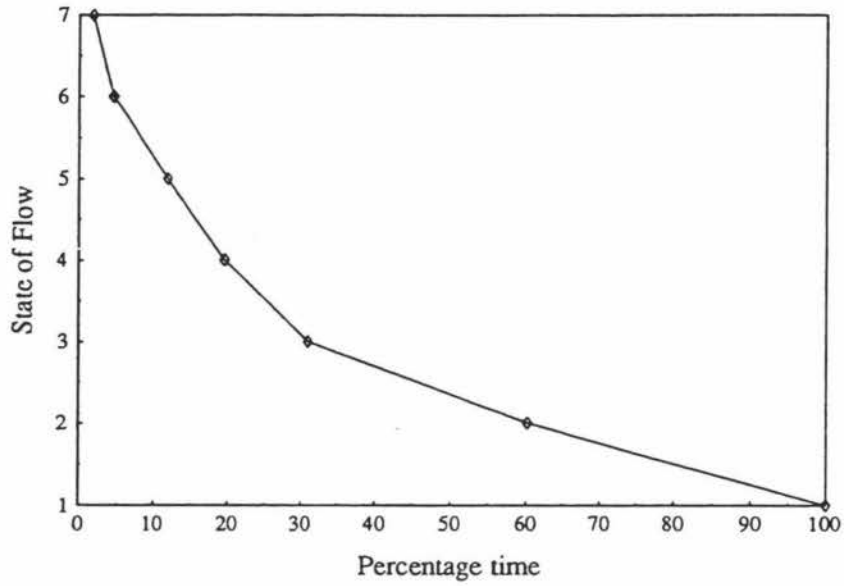

Fig. 4.14 Winter Flow Duration curve. Kiwitea Stream.

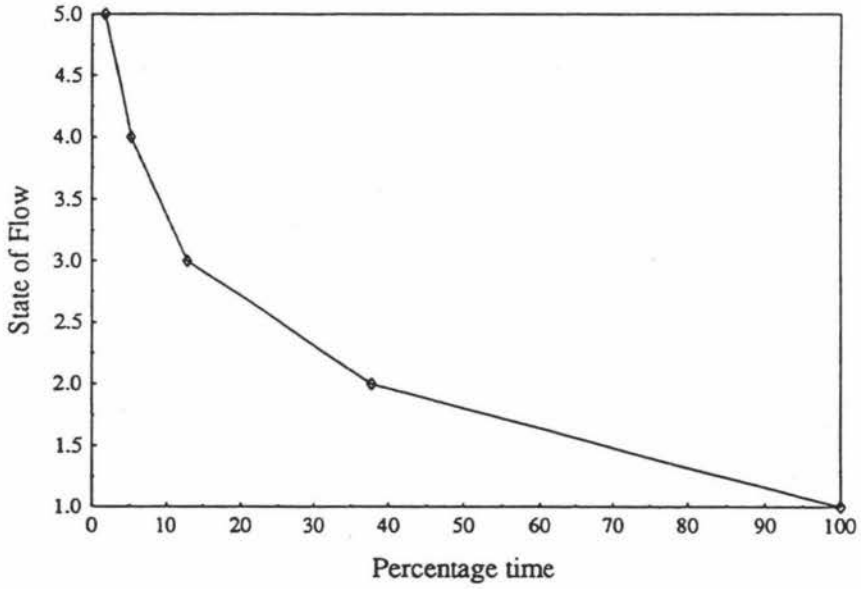

Fig. 4.15 Summer Flow Duration curve. Kiwitea Stream.

4.3.2 **Transition Probability Matrix**

The conditional probability that a state of streamflow at time t+1 will be in state 'j' given that at time t the streamflow was in state 'i', for all j and i over given states of streamflow were estimated. These probabilities are the elements of the so called Transition Probability Matrix (TPM) determined by using the calibration data.

The elements of the Transition Probability Matrices were estimated according to the method of maximum likelihood (Appendix I). The ratio n_{ij}/n_i is where n_{ij} represents the number of transitions from streamflow state i to j in one step and n_i is the number of times the streamflow is in state i. The values of n_{ij} and n_i were determined by a computer-aided search. As the Markov chain evolves in time, the frequencies of states in a given sequence of the streamflow states, X_t, are given in Tables 4.11, 4.14, 4.17, 4.20, 4.23 and 4.26.

Steady state transition probability vectors, where the probabilities represent the unconditional distribution of states, were also determined. For example, if we were to measure the streamflow at any given time of a season the chance of recording a value in a given state will be governed by the steady state probability vector.

4.3.2.1 **Transition Probability Matrix: Akitio River at Weber.**

The distribution of the transition probabilities in the Transition Probability Matrix, Table 4.12 suggests that in winter once a certain state of flow is attained, it tends to persist. This is more pronounced in low and high states of flow because of the high probabilities of maintaining the same states. For example, state 6, which is the flood state, has a probability of over 91% of maintaining that high state (state 6 or 5). Likewise low state 1 tends to persist as a low state 1 and 2 with over 93% probability.

The summer Transition Probability Matrix (Table 4.15) has a significant number of zero entries, which suggests that some one-step transitions are not possible, particularly those

transitions from high to low states (corresponding to the recession part of the hydrograph).

Table 4.13 and Table 4.16 give the steady state probabilities of streamflows over winter and summer months respectively. The calculations of expected states of flow give the mean seasonal states to be above state 2 during winter months and 1 during summer.

Table 4.11 Winter streamflow state transition (St_i -> St_j) frequencies. Akitio River.

St_i/St_j	1	2	3	4	5	6
1	879	26	11	26	11	18
2	72	27	4	7	5	5
3	10	17	6	5	4	4
4	6	43	15	27	13	14
5	1	6	11	47	17	12
6	2	1	0	6	43	49

Table 4.12 Winter Transition Probability Matrix. Akitio River.

St_i/St_j	1	2	3	4	5	6
1	0.905	0.027	0.011	0.027	0.011	0.019
2	0.600	0.225	0.033	0.058	0.042	0.042
3	0.217	0.370	0.130	0.109	0.087	0.087
4	0.051	0.364	0.127	0.229	0.110	0.119
5	0.011	0.064	0.117	0.500	0.181	0.128
6	0.020	0.010	0.000	0.059	0.426	0.485

Table 4.13 Winter steady state transition probability vector. Akitio River.

St_i	1	2	3	4	5	6
$p[St_i]$	0.667	0.083	0.032	0.082	0.065	0.072

Table 4.14 Summer streamflow state transition (St_i -> St_j). Akitio River.

St_i/St_j	1	2	3	4	5	6	7
1	1108	34	7	3	1	4	1
2	50	98	5	4	3	1	0
3	0	23	16	1	3	2	1
4	0	5	16	9	1	2	1
5	0	1	2	16	5	0	1
6	0	0	0	1	9	2	4
7	0	0	0	0	3	5	3

Table 4.15 Summer Transition Probability Matrix. Akitio River.

St_i/St_j	1	2	3	4	5	6	7
1	0.957	0.029	0.006	0.003	0.001	0.003	0.001
2	0.311	0.609	0.031	0.025	0.019	0.006	0.000
3	0.000	0.500	0.348	0.022	0.065	0.043	0.022
4	0.000	0.147	0.471	0.265	0.029	0.059	0.029
5	0.000	0.040	0.080	0.640	0.200	0.000	0.040
6	0.000	0.000	0.000	0.063	0.563	0.125	0.250
7	0.000	0.000	0.000	0.000	0.273	0.455	0.273

Table 4.16 Summer steady state transition probability vector.
Akitio River.

St_i	1	2	3	4	5	6	7
$p[St_i]$	0.603	0.251	0.035	0.018	0.010	0.006	0.017

4.3.2.2 **Transition Probability Matrix. Makakahi River at Hamua.**

From the probability distribution in the Transition Probability Matrix, in Table 4.18 it is evident that other than flood and low states, for every state the most probable next state is 2. For example, the chances that state 3 is followed by 2 is about 65% while maintaining state 3 itself the chances are 11%. The probability that the state of flow will change from state 4 to 2 is 43% but to maintain state 4 the probability is 33%. Also, some one-step transitions are not possible especially from high to low states of flow. The system seems to be dynamic in the intermediate states while persistence is more marked in low and flood states of flow.

The summer Transition Probability Matrix, Table 4.21 shows that low states of flow have a greater chance of persistence than higher states of flow. All the non-flood states of flow in the last column have very little chance of attaining a flood state in a one time-step progression; hence flash-flood events are not very likely.

Tables 4.19 and 4.22 present the seasonal steady state probability vectors. During summer about 97% of the time is flood free compared with 85% of winter time.

Table 4.17 Winter streamflow state transition (St_i -> St_j). Makakahi River.

St_i/St_j	1	2	3	4	5	6
1	524	43	8	6	7	21
2	83	140	7	10	3	20
3	2	44	8	3	3	8
4	0	21	16	4	0	8
5	0	11	8	3	2	12
6	0	4	21	23	21	107

Table 4.18 Winter Transition Probability Matrix. Makakahi River.

St_i/St_j	1	2	3	4	5	6
1	0.863	0.068	0.013	0.010	0.011	0.033
2	0.316	0.532	0.027	0.038	0.011	0.076
3	0.029	0.647	0.118	0.044	0.044	0.118
4	0.000	0.429	0.327	0.082	0.100	0.163
5	0.000	0.306	0.222	0.083	0.056	0.333
6	0.000	0.023	0.119	0.131	0.119	0.608

Table 4.19 Winter steady state transition probability vector. Makakahi River.

St_i	1	2	3	4	5	6
$P[St_i]$	0.494	0.213	0.062	0.047	0.037	0.145

Table 4.20 Summer streamflow state transition (St_i -> St_j). Makakahi River.

St_i/St_j	1	2	3	4	5	6
1	683	29	9	7	3	6
2	51	114	7	4	5	5
3	2	37	21	4	2	5
4	1	3	23	5	3	2
5	0	4	8	7	1	1
6	0	0	3	10	7	16

Table 4.21 Summer Transition Probability Matrix. Makakahi River.

St_i/St_j	1	2	3	4	5	6
1	0.927	0.039	0.012	0.009	0.004	0.008
2	0.273	0.610	0.037	0.021	0.027	0.027
3	0.028	0.521	0.296	0.056	0.028	0.070
4	0.027	0.081	0.622	0.135	0.081	0.054
5	0.000	0.190	0.381	0.333	0.048	0.048
6	0.000	0.000	0.083	0.278	0.194	0.444

Table 4.22 Summer steady state transition probability vector. Makakahi River.

St_i	1	2	3	4	5	6
$P[St_i]$	0.649	0.161	0.060	0.031	0.018	0.029

4.3.2.3 **Transition Probability Matrix. Kiwitea Stream**

Tables 4.24 and 4.27 give the Transition Probability Matrices for the Kiwitea Stream during the winter and summer months respectively. There are some impossible one time-step transitions here. For example, during winter states of flow 4 up to 7, the transition probabilities to lower states tend to be zero. Unlike the Akitio and Makakahi Rivers, the likelihood of flooding for the Kiwitea Stream is relatively small during winter months and non-existent in summer.

The steady state transition probability vectors are given in Tables 4.25 and 4.28. The winter mean expected state of flow is state 2 from the probability distribution in Table 4.25. Likewise state 1 is the expected summer state of flow (Table 4.28).

Table 4.23 Winter streamflow state transition (St_i -> St_j). Kiwitea Stream.

St_i/St_j	1	2	3	4	5	6	7
1	580	40	4	3	1	0	2
2	48	338	30	15	22	4	6
3	1	82	70	13	8	5	2
4	0	2	62	36	13	6	3
5	2	1	14	49	37	11	3
6	0	0	0	3	28	10	2
7	0	0	0	3	8	7	11

Table 4.24 Winter Transition Probability Matrix. Kiwitea Stream.

St_i/St_j	1	2	3	4	5	6	7
1	0.919	0.063	0.006	0.005	0.002	0.000	0.003
2	0.104	0.730	0.065	0.032	0.048	0.009	0.013
3	0.006	0.453	0.387	0.072	0.044	0.028	0.011
4	0.000	0.016	0.508	0.295	0.107	0.049	0.025
5	0.017	0.009	0.120	0.419	0.316	0.094	0.026
6	0.000	0.000	0.000	0.071	0.651	0.233	0.047
7	0.000	0.000	0.000	0.103	0.276	0.241	0.379

Table 4.25 Winter steady state transition probability vector. Kiwitea Stream.

St_i	1	2	3	4	5	6
$P[St_i]$	0.396	0.289	0.113	0.077	0.074	0.028

Table 4.26 Summer streamflow state transition (St_i -> St_j). Kiwitea Stream.

St_i/St_j	1	2	3	4	5
1	953	77	14	6	3
2	99	277	35	9	2
3	0	66	49	11	5
4	0	0	34	17	7
5	1	1	0	15	12

Table 4.27 Summer Transition Probability Matrix. Kiwitea Stream.

St_i/St_j	1	2	3	4	5
1	0.905	0.073	0.013	0.006	0.003
2	0.235	0.656	0.083	0.021	0.005
3	0.000	0.500	0.371	0.083	0.038
4	0.000	0.000	0.586	0.293	0.121
5	0.034	0.034	0.000	0.517	0.444

Table 4.28 Summer steady state transition probability vector. Kiwitea Stream.

St_i/St_j	1	2	3	4	5
$P[St_i]$	0.597	0.238	0.076	0.034	0.018

4.3.3 **Model performance quantification**

The quantification of the model performance is based on the two criteria of the objective function, which was evaluated under different model application procedures. An objective function graph is meant to provide the relevant facts required to make an informed decision when considered together with other decisive factors. In this case the preference of accepting more false alarms than misses, and bearing in mind the desire to simultaneously minimize both likelihoods was incorporated in the objective function graphs. On the objective function graphs (Figures 4.16 through 4.35) therefore, the non-dominated points lying in the region to the right of the line P(Ms) = P(FA) are the points to be considered. These non-dominated points in combination with their corresponding p_0 probabilities, for making a warning decision, are selected to quantify the model performance.

The evaluation of the two criteria-function each time the probability p_0 is varied on interval [0,1] gives sets of corresponding p_0 values and the objective values in terms of points (P(FA), P(Ms)). Under the preference of accepting more false alarms than misses, the most suitable point is selected from the calibration graph and its corresponding p_0 is found in the table of objective function values. This point corresponding to p_0 in the table of verification objective function values, has to be equal to or better than the calibration point in terms of the objective function for quantifying the model performance. The model performance is tested for the two approaches (ThFc and MPE).

When the model performance is assessed using the threshold forecasts approach, trade-offs between false alarms and misses are considered as the flood probability is varied on [0,1]. At each point the objective function (equations (6) and (7)) is calculated after determining the nHf, nFA, nHnf and nMs. These are counts from a data set (series X_t) under the following cases:

> Case 1: When the transition probability p[i,q] (the last column of the transition probability matrix) is at least p_0 and the observed state corresponding to time t+1 is a flood state then nHf is counted - otherwise nFA is counted.
>
> Case 2: When p[i,q] is less than p_0 and the observed state in the series at time t+1 is not the flood state then nHnf is counted, else nMs is counted. Each pair [P(FA),P(Ms)] represents a point in the objective function space. For example Tables 4.27, 4.34 and 4.35 present "pay-off" values which determine the objective function values as p_0 is varied for calibration and verification data sets.

Similarly, with the model performance assessment using the "most probable event" forecasts, at each point as the probability is varied on the interval [0,1] the objective function (Equations (7) and (8)) is calculated after determining the nHf, nFA, nHnf and nMs. These counts are made from a data set (series X_t) under the following

considerations:

Case 1: When the highest transition probability p[i,j] (from state i at time t to state j at time t+1) is equal or greater than p_0 and state j is the flood state then nHf is counted, otherwise nFA is counted.

Case 2: When p[i,j] is less than p_0 and state j is not the flood state then nHnf is counted else nMs is counted. Each pair [P(FA), P(Ms)] represents a point in the objective function space. For example Tables 4.29, 4.30, 4.31, 4.32, 4.33 and 4.34 present trade-offs between false alarms and misses at different pairs of objective function values, [P(FA), P(Ms)].

4.3.3.1 **Model quantification for the Akitio River**

Tests of model performance using the "threshold forecasts approach" were made with data sets from the Akitio River at Weber. The objective function values and trade-offs were evaluated as the threshold probability p_0 was varied on the interval [0, 1]. The results are listed in Tables 4.29 and 4.30 for winter and Tables 4.33 and 4.34 for summer. Plots of the objective function (P(Ms) v^s P(FA)) for winter calibration and verification data sets are shown in Figures 4.16 and 4.17 respectively. The plots for the summer data sets are shown in Figures 4.20 and 4.21.

In the sense of multi-objective analysis, all points on these graphs are non-dominated solutions (see Equation 1). As p_0 is varied from 0 to 1, the probability of issuing a false alarm decreases while the probability of a miss increases or does not change.

The model performance testing procedure was repeated using the "most probable event forecasts", the results of which are shown in Tables 4.31 and 4.32 for winter calibration and verification data sets. Figures 4.18 and 4.19 show their respective objective function plots. Again all points on this graph are non-dominated points.

Figures 4.16 and 4.17 can be used to quantify the model performance using the ThFc approach. The non-dominated points are **a**, **b**, **c**, **d**, **e**, **f**, and **g**. Every point from point **a** to **g** corresponds to a value of p_0 in Tables 4.29 and 4.30. Under the preference of accepting more false alarms than misses, the most suitable point lies in the region which is to the right of the line P(Ms) = P(FA). To simultaneously minimize both P(FA) and P(Ms), the most suitable point is **f**(0.2907, 0.2020) which is subjectively selected because both P(FA) and P(Ms) are both small. This point corresponds to the appropriate probability interval p_0 [0.02 , 0.049]. Using this range of p_0 for verification, the objective function $H(p_0)$ corresponds to point **f**(0.2719, 0.1667) on Figure 4.17. The results of this evaluation quantifies the model by setting the appropriate flood warning probability p_0.

For summer calibration (see Fig. 4.20) the point **f**(0.0806, 0.000) is the most suitable point and corresponds to p_0 in the interval [0.01, 0.059] in Table 4.33. On the verification plot this p_0 corresponds to point **f**(0.1368, 0.0000) (see Fig. 4.21 and Table 4.34).

When the model performance is tested using the "most probable event forecasts" approach, the results are depicted in Figure 4.18, and point **c**(0.7783, 0.7200) is the most suitable calibration point, and corresponds to p_0 in the interval [0.51, 0.609] in Table 4.31 which corresponds to **c**(0.8000, 0.8333) in the verification Table 4.32 and on the verification graph (Fig. 4.19). The probability of a miss and the probability of a false alarm might be considered too high for the model to be acceptable for flood prediction. The point **c** on the verification does not meet the desired preference as the probability of a miss is greater than the probability of a false alarm.

Similarly, the model performance test for the summer is depicted in Figures 4.22 for calibration and 4.23 for verification, although the probabilities of false alarms and misses are too high. It also shows that the calibration point **c** in the feasible region is out of the region in the verification graph (the objective function non-dominated points are given in Table A.1).

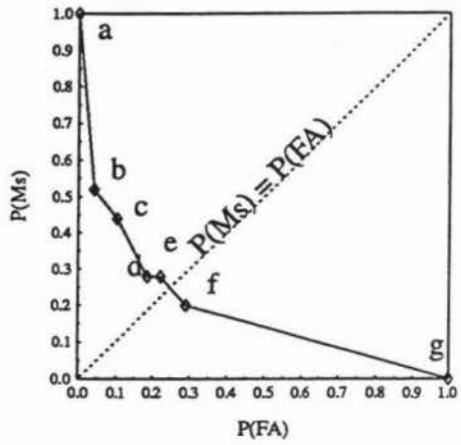

Fig. 4.16 ThFc Objective function. Akitio, winter calibration.

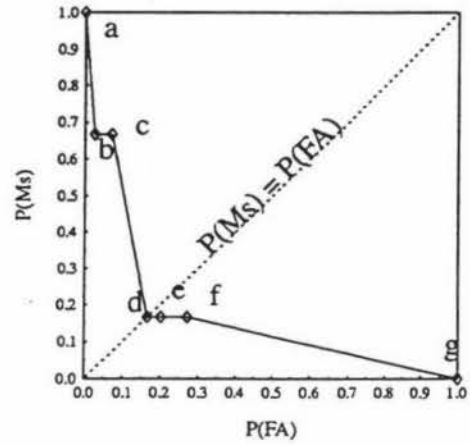

Fig. 4.17 ThFc Objective function. Akitio, winter verification.

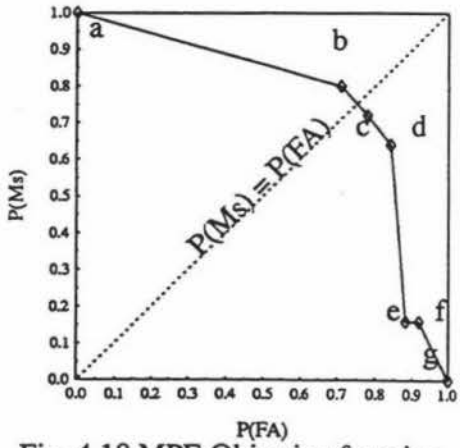

Fig. 4.18 MPE Objective function. Akitio, winter calibration.

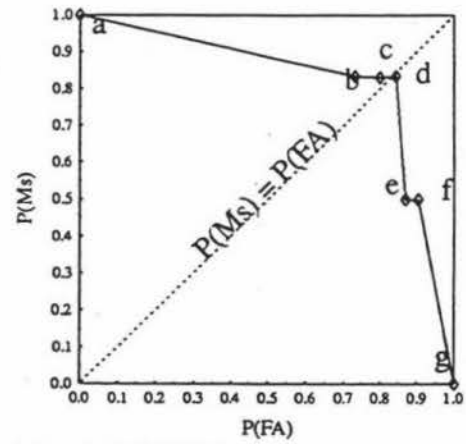

Fig. 4.19 MPE Objective function. Akitio, winter verification.

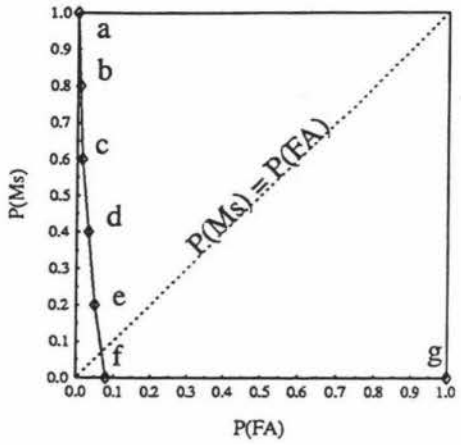

Fig. 4.20 ThFc objective function. Akitio, summer calibration.

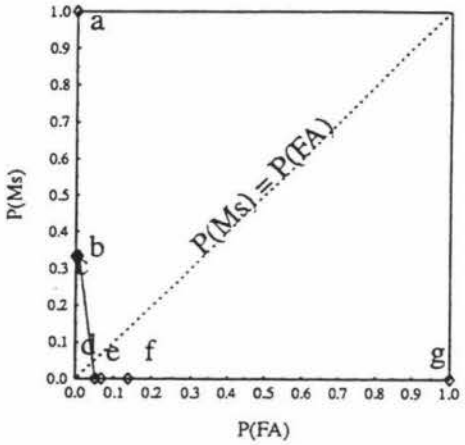

Fig. 4.21 ThFc Objective function. Akitio, summer verification.

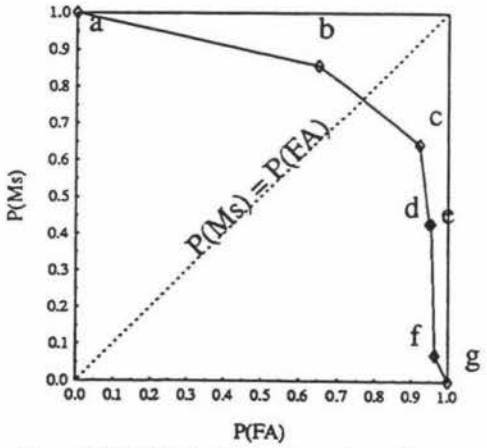

Fig. 4.22 MPE Objective function. Akitio, summer calibration.

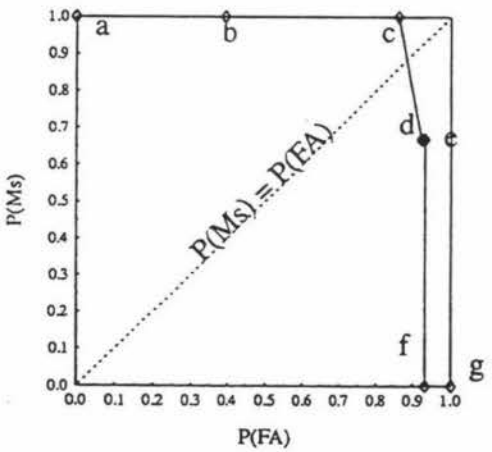

Fig. 4.23 MPE Objective function. Akitio, summer verification.

Table 4.29 ThFc Pay-off values and Objective function points. Akitio River, winter calibration.

p_0 / (Point)	nHf	nMs	nFA	nHnf	P(FA)	P(Ms)
0.00 - 0.019 (g)	50	0	681	0	1.0000	0.0000
0.02 - 0.049 (f)	40	10	698	483	0.2907	0.2020
0.05 - 0.089 (e)	36	14	151	530	0.2217	0.2800
0.09 - 0.119 (d)	36	14	126	555	0.1850	0.2800
0.12 - 0.129 (c)	28	22	70	611	0.1028	0.4400
0.13 - 0.489 (b)	24	26	28	653	0.0411	0.5200
0.49 - 1.000 (a)	0	50	0	681	0.0000	1.0000

Table 4.30 ThFc Pay-off values and Objective function points. Akitio River, winter verification.

p_0 / (Point)	nHf	nMs	nFA	nHnf	P(FA)	P(Ms)
0.00 - 0.019 (g)	6	0	114	0	1.0000	0.0000
0.02 - 0.049 (f)	5	1	31	83	0.2719	0.1667
0.05 - 0.089 (e)	5	1	23	91	0.2018	0.1667
0.09 - 0.119 (d)	5	1	19	95	0.1667	0.1667
0.12 - 0.129 (c)	2	4	8	106	0.0702	0.6667
0.13 - 0.489 (b)	2	4	3	111	0.0263	0.6667
0.49 - 1.000 (a)	0	6	0	114	0.0000	1.000

Table 4.31 MPE Pay-off values and Objective function points. Akitio River, winter calibration.

p_0 / (Point)	nHf	nMs	nFA	nHnf	P(FA)	P(Ms)
0.00 - 0.369 (g)	50	0	680	0	1.0000	0.0000
0.37 - 0.379 (f)	42	8	630	55	0.9178	0.1600
0.38 - 0.489 (e)	42	8	600	80	0.8811	0.1600
0.49 - 0.509 (d)	18	32	570	110	0.8399	0.6400
0.51 - 0.609 (c)	14	36	530	150	0.7783	0.7200
0.61 - 0.909 (b)	10	40	480	200	0.7093	0.8000
0.91 - 1.000 (a)	0	50	0	680	0.0000	1.0000

Table 4.32 MPE Pay-off values and Objective function points. Akitio River, winter verification.

p_0 / (Point)	nHf	nMs	nFA	nHnf	P(FA)	P(Ms)
0.00 - 0.369 (g)	6	0	110	0	1.0000	0.0000
0.37 - 0.379 (f)	3	3	100	11	0.9043	0.5000
0.38 - 0.489 (e)	3	3	100	15	0.8696	0.5000
0.49 - 0.509 (d)	1	5	97	18	0.8435	0.8333
0.51 - 0.609 (c)	1	5	92	23	0.8000	0.8333
0.61 - 0.909 (b)	1	5	84	31	0.7304	0.8333
0.91 - 1.000 (a)	0	6	0	110	0.0000	1.0000

Table 4.33 ThFc Pay-off values and Objective function points. Akitio River, summer calibration.

p_0	Nhf	nMs	nFA	nHnf	P(FA)	P(Ms)
0.00 - 0.009 (g)	5	0	720	0	1.0000	0.0000
0.01 - 0.059 (f)	5	0	58	662	0.0806	0.0000
0.06 - 0.069 (e)	4	1	36	684	0.0500	0.2000
0.07 - 0.109 (d)	3	2	23	697	0.0319	0.4000
0.11 - 0.119 (c)	2	3	10	710	0.0139	0.6000
0.12 - 0.469 (b)	1	4	5	715	0.0060	0.8000
0.47 - 1.000 (a)	0	5	0	720	0.0000	1.0000

Table 4.34 ThFc Pay-off values and Objective function points. Akitio River, summer verification.

p_0 / (Point)	nHf	nMs	nFA	nHnf	P(FA)	P(Ms)
0.00 - 0.009 (g)	3	0	117	0	1.0000	0.0000
0.01 - 0.059 (f)	3	0	16	101	0.1368	0.0000
0.06 - 0.069 (e)	3	0	8	109	0.0684	0.0000
0.07 - 0.109 (d)	3	0	6	111	0.0513	0.0000
0.11 - 0.119 (c)	2	1	1	116	0.0085	0.3333
0.12 - 0.469 (b)	2	1	0	117	0.0000	0.3333
0.47 - 1.000 (a)	0	3	0	117	0.0000	1.0000

4.3.3.2 **Model quantification for the Makakahi River**

The results of the threshold forecasts approach, using the model performance assessment in terms of objective function, are shown in Tables 4.35 and 4.36 for winter calibration and verification and Tables 4.39 and 4.40 for the summer. Plots of these values are given in Figures 4.24 and 4.25 (winter) and Figures 4.28 and 4.29 (summer).

All points on the graphs are non-dominated solutions. As p_0 is varied from 0 to 1, the probability of issuing a false alarm decreases while the probability of a miss increases.

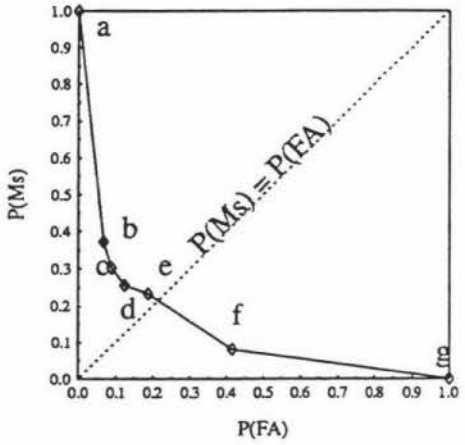

Fig. 4.24 ThFc Objective function. Makakahi, winter calibration.

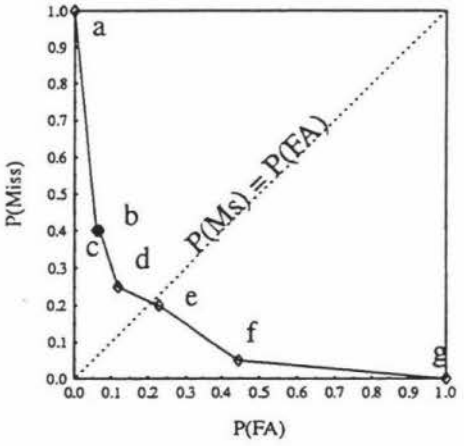

Fig. 4.25 ThFc Objective function. Makakahi, winter verification.

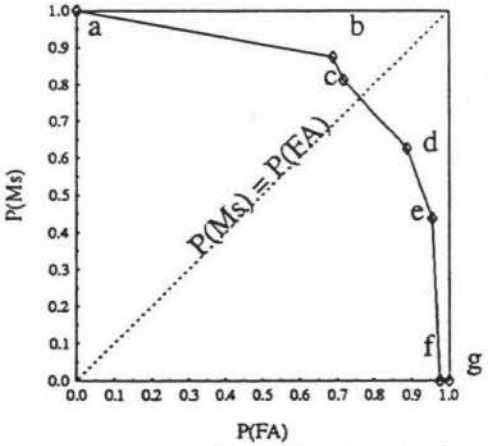

Fig. 4.26 MPE Objective function. Makakahi, winter calibration.

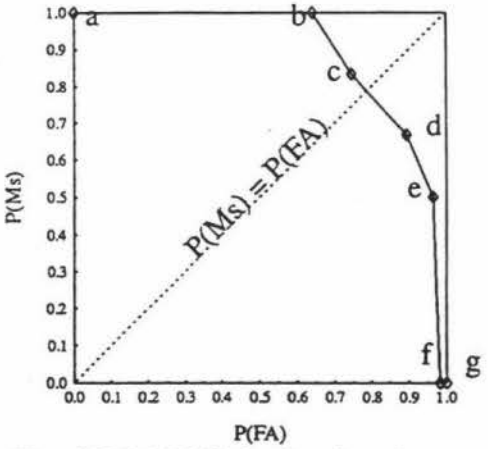

Fig. 4.27 MPE Objective function. Makakahi, winter verification.

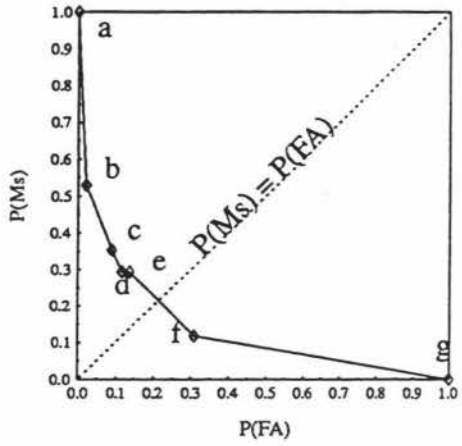

Fig. 4.28 ThFc Objective function. Makakahi, summer calibration.

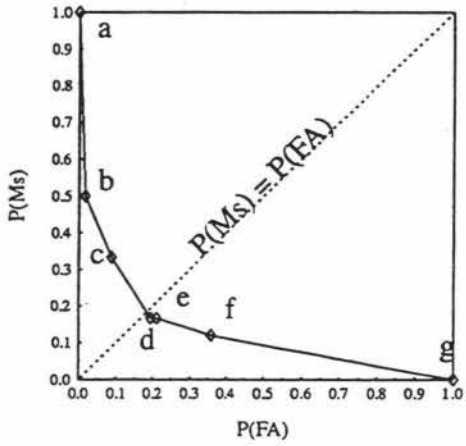

Fig. 4.29 ThFc Objective function. Makakahi, summer verification.

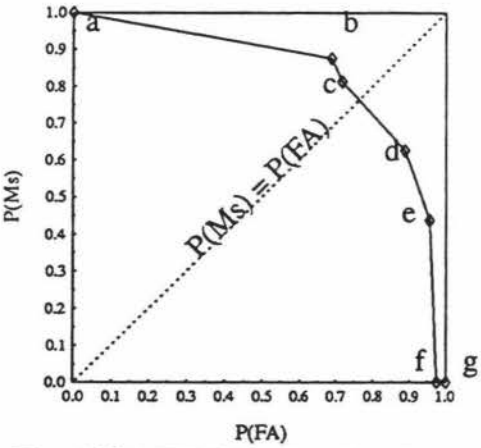

Fig. 4.30 MPE Objective function. Makakahi, summer calibration.

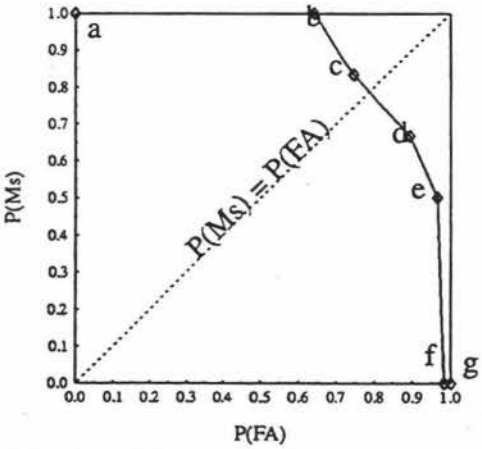

Fig. 4.31 MPE Objective function. Makakahi, summer verification.

As depicted in Figures 4.24 the performance of the model is quantified from point **f**(0.4149, 0.0814) being the most suitable calibration point corresponding to p_0 = [0.04, 0.079] in Table 4.35. In the verification (Table 4.36), the calibration p_0 interval corresponds to **f**(0.4500, 0.0500) on the verification graph (Fig. 4.25). Although the probability of a miss is fairly small (0.05), the probability of a false alarm (0.45) might be too high for the model to be accepted.

From the evaluation of the model objective function with summer data sets, the graphs in Figures 4.28 and 4.29 show the functions for calibration and verification respectively. Point **f**(0.3112, 0.1250) on the calibration plot is the most suitable point and corresponds to p_0 in interval [0.01, 0.029] as shown in Table 4.39. In Table 4.40 this interval of p_0 corresponds to point **f**(0.3596 0.0000) on the verification graph. Although the probabilities of misses zero, the probability of false alarms is significantly high therefore the model is unlikely to be acceptable.

When the model performance is tested using the "most probable event forecasts", Tables 4.37 and 4.38 show the objective function values and their respective trade-offs. Figures 4.26 and 4.27 are the objective function plots. All points on the graph are non-dominated ones as well.

It shows that **d**(0.7170, 0.2674) is the most suitable point on the objective function graph for the winter calibration period and corresponds to p_0 in the interval [0.54, 0.609] (Table 4.37). This p_0 on the verification function table corresponds to point **d**(0.7228, 0.3000) (Table 4.38). In this case the probability of a false alarm of 0.7228 and 0.3000 for a miss, evidently gives probabilities which are too high for the model to be acceptable. Figures 4.30 and 4.31 show the same objective function character for summer as in winter, likewise suggesting rejection of the model.

Table 4.35 ThFc Pay-off values and Objective function points.
Makakahi River, winter calibration.

p_0 / (Point)	nHf	nMs	nFA	nHnf	P(FA)	P(Ms)
0.00 - 0.039 (g)	86	0	523	0	1.0000	0.0000
0.04 - 0.079 (f)	79	7	217	306	0.4149	0.0814
0.08 - 0.119 (e)	66	20	98	425	0.1874	0.2326
0.12 - 0.169 (d)	64	22	65	458	0.1243	0.2558
0.17 - 0.339 (c)	60	26	47	476	0.0899	0.3028
0.34 - 0.609 (b)	54	32	36	487	0.0688	0.3721
0.61 - 1.000 (a)	0	86	0	523	0.0000	1.0000

Table 4.36 ThFc Pay-off values and Objective function points.
Makakahi River, winter verification.

p_0 / (Point)	nHf	nMs	nFA	nHnf	P(FA)	P(Ms)
0.00 - 0.039 (g)	20	0	100	0	1.0000	0.0000
0.04 - 0.079 (f)	19	1	45	55	0.4500	0.0500
0.08 - 0.119 (e)	16	4	23	77	0.2300	0.2000
0.12 - 0.169 (d)	15	5	12	88	0.1200	0.2500
0.17 - 0.339 (c)	12	8	7	93	0.0700	0.4000
0.34 - 0.609 (b)	12	8	6	94	0.0600	0.4000
0.61 - 1.000 (a)	0	20	0	100	0.0000	1.0000

Table 4.37 MPE Pay-off values and Objective function points. Makakahi River, winter calibration.

p_0 / (Point)	nHf	nMs	nFA	nHnf	P(FA)	P(Ms)
0.00 - 0.339 (g)	86	0	520	0	1.0000	0.0000
0.34 - 0.429 (f)	86	6	510	11	0.9790	0.0698
0.43 - 0.539 (e)	76	10	490	29	0.9446	0.1163
0.54 - 0.609 (d)	63	23	380	150	0.7170	0.2674
0.61 - 0.649 (c)	9	77	340	180	0.6482	0.8953
0.65 - 0.869 (b)	7	79	310	220	0.5851	0.9186
0.87 - 1.000 (a)	0	86	0	520	0.0000	1.0000

Table 4.38 MPE Pay-off values and Objective function points. Makakahi River, winter verification.

p_0 / (Point)	nHf	nMs	nFA	nHnf	P(FA)	P(Ms)
0.00 - 0.339 (g)	20	0	100	0	1.0000	0.0000
0.34 - 0.429 (f)	20	0	100	1	0.9901	0.0000
0.43 - 0.539 (e)	17	3	95	6	0.9406	0.1500
0.54 - 0.609 (d)	14	6	73	28	0.7228	0.3000
0.61 - 0.649 (c)	2	18	67	34	0.6634	0.9000
0.65 - 0.869 (b)	1	19	56	45	0.5545	0.9500
0.89 - 1.000 (a)	0	20	0	100	0.0000	1.0000

Table 4.39 ThFc Pay-off values and Objective function points. Makakahi River, summer calibration.

p_0 /(Point)	nHf	nMs	nFA	nHnf	P(FA)	P(Ms)
0.00 - 0.009 (g)	16	0	527	0	1.0000	0.0000
0.01 - 0.029 (f)	14	2	164	363	0.3112	0.1250
0.03 - 0.049 (e)	11	5	74	453	0.1404	0.3125
0.05 - 0.059 (d)	11	5	61	466	0.1157	0.3125
0.06 - 0.079 (c)	10	6	46	481	0.0873	0.3750
0.08 - 0.449 (b)	7	9	10	517	0.0190	0.5625
0.45 - 1.000 (a)	0	16	0	527	0.0000	1.0000

Table 4.40 ThFc Pay-off values Objective and function points. Makakahi River, summer verification.

p_0 / (Point)	nHf	nMs	nFA	nHnf	P(FA)	P(Ms)
0.00 - 0.009 (g)	6	0	114	0	1.0000	0.0000
0.01 - 0.029 (f)	6	0	41	73	0.3596	0.0000
0.03 - 0.049 (e)	5	1	24	90	0.2105	0.1667
0.05 - 0.059 (d)	5	1	22	92	0.1930	0.1667
0.06 - 0.079 (c)	4	2	10	104	0.0877	0.3333
0.08 - 0.449 (b)	3	3	2	112	0.0175	0.50001.
0.45 - 1.000 (a)	0	6	0	114	0.0000	0000

4.3.3.3 **Model quantification for the Kiwitea Stream**

Tables 4.41 and 4.42 show the threshold forecasts objective function plots (P(Ms) v^s P(FA)) for winter calibration and verification. No summer objective function values were considered since there were no flood events in the summer season. In Figures 4.32 and 4.33 all points are non-dominated solutions.

From the calibration objective function graph the most suitable point is **e**(0.5944, 0.0000) and corresponds to p_0 in [0.01, 0.019] in Table 4.41. In Table 4.42, that p_0 interval corresponds to **e**(0.8750, 0.0000) on the verification graph. In this case although the probability of a miss is zero, the probability of a false alarm is too high for the model to be acceptable.

The model performance when using the "most probable event forecasts" on the Kiwitea Stream results are presented in Table 4.43 and 4.44. These results illustrate a rejection of the model on the basis of the multi-objective criteria.

From Figure 4.34 the most suitable point is **d**(0.7266, 0.6154) which corresponds to p_0 in interval [0.51, 0.659] in Table 4.43. In Table 4.44 the interval [0.51, 0.659] corresponds the objective function values **d**(0.5690, 0.5000) on the verification graph in

Figure 4.35. Again the probabilities for both false alarms and misses seem to be too high for the model to be suitable.

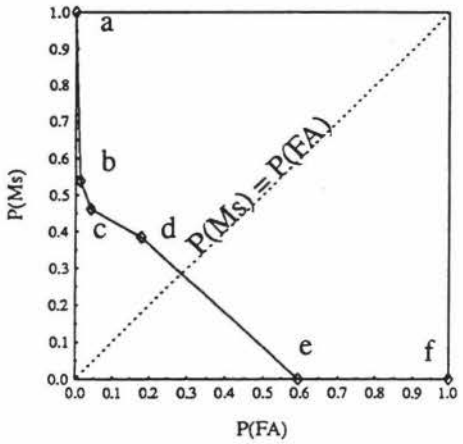

Fig. 4.32 ThFc Objective function. Kiwitea, winter calibration.

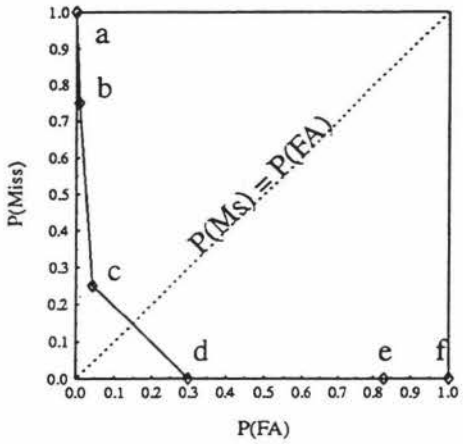

Fig. 4.33 ThFc Objective function. Kiwitea, winter verification.

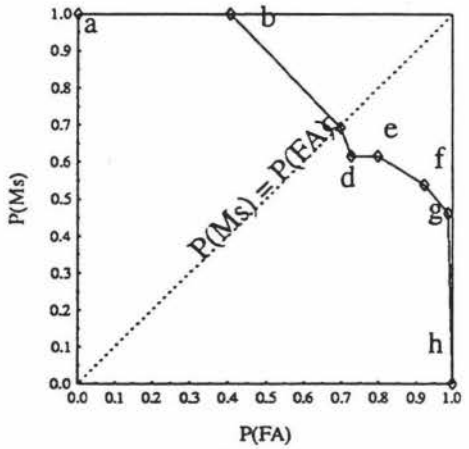

Fig. 4.34 MPE Objective function. Kiwitea, winter calibration.

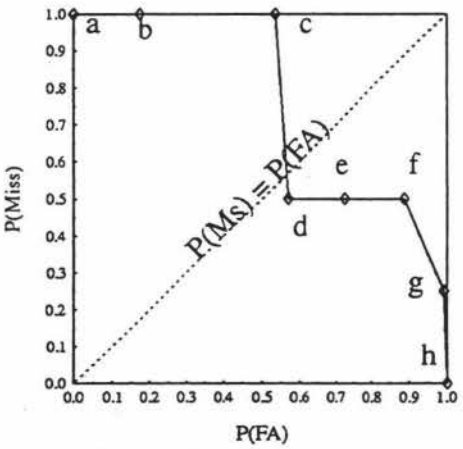

Fig. 4.35 MPE Objective function. Kiwitea, winter verification.

Table 4.41 ThFc Pay-off values Objective and function points. Kiwitea Stream, winter calibration.

p_0 / (Point)	nHf	nMs	nFA	nHnf	P(FA)	P(Ms)
0.00 - 0.009 (f)	13	0	779	0	1.0000	0.0000
0.01 - 0.019 (e)	13	0	463	316	0.5944	0.0000
0.02 - 0.029 (d)	8	5	139	640	0.1784	0.3846
0.03 - 0.049 (c)	7	6	32	747	0.0411	0.4615
0.05 - 0.379 (b)	6	7	10	769	0.0128	0.5385
0.38 - 1.000 (a)	0	13	0	779	0.0000	0.1000

Table 4.42 ThFc Pay-off values Objective function points. Kiwitea Stream, winter verification.

p_0 / (Point)	nHf	nMs	nFA	nHnf	P(FA)	P(Ms)
0.00 - 0.009 (f)	4	0	56	0	1.0000	0.0000
0.01 - 0.019 (e)	4	0	49	7	0.8750	0.0000
0.02 - 0.029 (d)	4	0	12	44	0.2143	0.0000
0.03 - 0.049 (c)	3	1	3	53	0.0536	0.2500
0.05 - 0.379 (b)	1	3	1	55	0.0179	0.7500
0.38 - 1.000 (a)	0	4	0	56	0.0000	1.0000

Table 4.43 MPE Pay-off values Objective function points. Kiwitea Stream, winter calibration.

p_0 / (Point)	nHf	nMs	nFA	nHnf	P(FA)	P(Ms)
0.00 - 0.379 (h)	13	0	780	0	1.0000	0.0000
0.38 - 0.419 (g)	7	6	770	10	0.9872	0.4615
0.42 - 0.459 (f)	6	7	720	61	0.9217	0.5385
0.46 - 0.509 (e)	5	8	620	160	0.7985	0.6154
0.51 - 0.659 (d)	5	9	570	210	0.7266	0.6154
0.66 - 0.739 (c)	4	9	540	230	0.6983	0.6923
0.74 - 0.919 (b)	0	13	320	460	0.4056	1.0000
0.92 - 1.000 (a)	0	13	0	780	0.0000	1.0000

Table 4.44 MPE Pay-off values and Objective function points. Kiwitea Stream, winter verification.

p_0 (Point)	P(FA)	P(Ms)
0.00 - 0.379 (h)	1.0000	0.0000
0.38 - 0.419 (g)	0.9914	0.2500
0.42 - 0.459 (f)	0.8879	0.5000
0.46 - 0.509 (e)	0.7241	0.5000
0.51 - 0.659 (d)	0.5690	0.5000
0.66 - 0.739 (c)	0.5345	1.0000
0.74 - 0.919 (b)	0.1724	1.0000
0.92 - 1.000 (a)	0.0000	1.0000

4.3.4 **Model performance quantification summary**

The model used two approaches to forecast a one time-step ahead state of streamflow, the threshold probability forecast (ThFc) approach and the Most Probable Event (MPE) forecast as defined in Chapter 3. Evaluation of an objective function with two criteria, namely the probability of a false alarm and the probability of a miss, is done by varying a threshold probability p_0 for making a decision to issue a flood warning or not. Tables 4.45, 4.46, 4.47 and 4.48 display the threshold flood warning probabilities p_0 and the

associated probabilities of false alarms P(FA) and probabilities of misses P(Ms) as the quantification of the model performance.

Table 4.45 ThFc selected objective function values (winter).

River	p_0	$H(p_0)$	
		P(FA)	P(Ms)
Akitio	0.02 - 0.049	0.2719	0.1667
Makakahi	0.04 - 0.079	0.4500	0.0500
Kiwitea	0.01 - 0.019	0.8750	0.0000

Table 4.46 ThFc selected objective function values (summer).

River	p_0	$H(p_0)$	
		P(FA)	P(Ms)
Akitio	0.01 - 0.059	0.1368	0.0000
Makakahi	0.01 - 0.029	0.3596	0.0000

Table 4.47 MPE selected objective function values (winter).

River	p_0	$H(p_0)$	
		P(FA)	P(Ms)
Akitio	0.51 - 0.609	0.8000	0.8300
Makakahi	0.54 - 0.609	0.7228	0.3000
Kiwitea	0.51 - 0.659	0.5690	0.5000

Table 4.48 MPE selected objective function values (summer).

River	p_0	$H(p_0)$	
		P(FA)	P(Ms)
Akitio	0.63 - 0.829	0.8632	1.0000
Makakahi	0.53 - 0.619	0.8889	0.6667

Using the threshold forecast approach the results showed that for the Akitio River in summer, at threshold probability p_0 in the interval [0.01, 0.059], the probability of a false alarm was 13.68% with no chance of a miss (P(Ms) = 0). In winter, p_0 was defined on the interval [0.02, 0.049] and the probability for false alarms was 27.19% and 16.67% for the misses. Depending on the costs assigned to the two events the model might to be acceptable.

With the threshold forecasts option the model performed rather poorly for the Makakahi River. Even though during both summer and winter seasons the probability of misses was small (0% and 5%), the probability for false alarms was high (35% and 45%).

For the Kiwitea Stream the analysis showed that no floods are expected during summer. In winter, making use of the threshold forecast approach, the model application showed the probability of false alarm to be as high as 87.50%.

The model application using the most probable event forecasts gave very high probabilities of both false alarms and misses. For example, when the model was tested for Akitio River winter floods, the false alarm probability was as high as 80% with a probability of 83% for a miss. Similarly for the Makakahi and Kiwitea, the probabilities for false alarms and misses are too high for the model to be acceptable.

The model seemed to perform best for the Akitio River, especially during summer flows, and could be related to the large variations in streamflows. On average, the Akitio River streamflows are very erratic with a coefficient of variation (Cv) over 3 while the Makakahi River and Kiwitea Stream have streamflow coefficients of variation which are less than 2. As postulated in Chapter 3 (Section 3.3), a Markov chain flow model assumes the streamflow process to be a phenomenon that varies as time advances, and the variation has to have a significant chance component (Alan F. K.,1990). Under this assumption the streamflow variations in the Akitio River are approximated by the model more closely than in the other two rivers. The performance of the model on the Akitio River data set compares well with the results of Yapo et al.(1993) using a Markov chain flow model on the Salt River (Arizona, U S A), a river with erratic streamflows.

Chapter 5

SUMMARY AND CONCLUSIONS

5.1 Summary

This study investigated a Markov chain flow model for its application as a simple short-term streamflow forecasting model. Daily mean streamflow values expressed in terms of states of flow were the only model input. In this approach forecasts are in terms of states of flow, and are based on the probability transition matrix (PTM) determined from the calibration data. Forecasts being in terms of states of flow, instead of single streamflow values, is a particular feature of this model.

Two types of model forecasts to examine the model performance were considered, particularly in forecasting floods. The two approaches are the Threshold Forecasts (ThFc) and the Most Probable Event (MPE) forecasts. The application of the model in flood forecasting has several options within the probabilistic framework for deciding whether to issue a flood warning or not. The concept of a threshold probability of a flood event occurrence (p_0) was introduced for a decision whether to issue a flood warning or not whenever the flood probability is not zero.

The model performance was quantified through a two criteria objective function restricted to one state of streamflow, "the flood state". The criteria are the probability of issuing a false alarm and the probability of a flood miss. The objective function was evaluated for every p_0 which was varied on the interval [0, 1]. Under the preference of accepting more false alarms than misses, the most acceptable combination of p_0 and the function values (P(FA), P(Ms)) were used to quantify the model. This provided an aid in determining whether the model was suitable enough for flood forecasting and warning purposes.

The results of the application of the model to three catchments in the southern North

Island illustrate how the performance of the model can be quantified. Depending on the relative costs assigned to false alarms and misses an informed decision can be made to use the model or not.

5.2 **Conclusion**

The performance of the Markov-chain flow model in short-term flood forecasting was found to be reasonably good when used for erratic (high Cv) streamflows, when evaluated in terms of the multi-objective function criteria. The model worked better with the threshold forecasts procedure than with the most probable event forecasts procedure.

The model could be a valuable tool for users like regional councils, especially those responsible for rivers and streams with erratic streamflows, a characteristic typical of eastern catchments in New Zealand. Although this study focuses the objective function to one streamflow state, floods, an objective function more conducive to river and reservoir management can be developed in which each criterion would be the probability of correct forecast within each streamflow state.

REFERENCES

Alan, F.K. 1990. Markov Processes. Chapter 2. In: Heyman D. P. and Sobel M. J.(eds). Stochastic Models. North-Holland.

Cecconic, G. 1988. Step-ahead state forecasting using streamflow observations. Agricultural-Water-Management. 13(2-4):169-183.

Haan C.T., Allen D.M. and Street J.O. 1976. A Markov model of daily rainfall, Water Resour. Res., 12(3), 443-449.

Haan, C.T. 1977. Statistical Methods in Hydrology. First Edition pp 302- 309.

Isaacson, D.L. 1976. Markov Chains Theory and Applications, 107 pp.,John Wiey, New York.

Jackson, B.B. 1975a. Markov mixture models for drought lengths. Water Resour. Res. 11(1):64-74.

Jackson, B.B. 1975b. Birth-death models for differential persistence. Water Resour. Res. 11(1):75-95.

Karlsson, M. and Yakowitz, S.T. 1987. Nearest-neighbour methods for nonparametric rainfall-runoff forecasting. Water Resources Res. 23(7):1300-1308.

Katz, R.W. 1981. On some criteria for estimating the order of a Markov chain. Technometrics 23(3):243-249.

Lettenmaier, D., Wood, E., and Parkinson, D. 1990. Operating the Seattle water system during the 1987 drought management and operations. Journal of AWWA. 55-60.

Minitab Inc. 1994, Minitab Reference Manual. Minitab Inc. USA.

Pearson C.P. and Jordan R.S., 1991. New Zealand Flood Forecasting Procedures and Reliability. Publication No. 25 of the Hydrology Centre, Christchurch.

Ramirez, T. and Bras, R. 1985. Conditional distributions of Neyman-Scott models for storm arrivals and their use in irrigation scheduling. Water Resource Res. 21(3):317-330.

Sorooshian, S. 1992. Hydrologic forecasting. Encyclopedia of Earth System Science. vol.2, pp 537-546. Academic, San Diego, California.

Smith, J.A. 1991. Long-range streamflow forecasting using nonparametric regression. Water Resources Bulletin.27(1): 39 -46.

Smith, J.A. 1989. Water supply yield analysis for the Washington metropolitan area. Journal of Water Resources Planning and Management, ASCE, 115(2):230-242.

Yakowitz, S.T. 1985. Markov flow models and the flood warning problem. Water Resour. Res. 21(5):81-88.

Yakowitz, S.T. 1979. A nonparametric model for daily river flow. Water Resour. Res. 15(5):1035-1043.

Yapo, P., Sorooshian, S., Gupta, V. 1993. A Markov chain flow model for flood forecasting. Water Resource Res. 29(7): 2427-2436.

Yevjevich, V. 1972. Probability and Statistics in Hydrology. First Edition.

Zielinski, P.A. 1991. On meaning of randomness in stochastic environmental models. Water Resour. Res. 29(7): 1607-1611.

APPENDICES

Appendix I: The Maximum Likelihood Method

Consider $\{X_t\}$ a Markov chain of order one and a case where the chain has two states, 1 and 2. As the chain evolves in time, a sequence of m observations is recorded where each observation represents a state of the Markov chain. From those m observations a matrix M is constructed as follows:

$$M = \begin{matrix} m11 & m12 \\ m21 & m22 \end{matrix}$$

Each entry of the matrix is the count of pairs (1,1), (1,2), (2,1) and (2,2). For example we can have 11 observations recorded sequentially as 2, 1, 2, 1, 2, 2, 1, 2, 1, 2, 2 which means the chain evolves in time from state 2 to state 1, state 1 to state 2, and so on. Thus the matrix M becomes

$$M = \begin{matrix} 0 & 4 \\ 4 & 2 \end{matrix}$$

Let $L(X_1, X_2, ..., X_m) = P_{11}^{m11} \times P_{12}^{m12} \times P_{21}^{m21} \times P_{22}^{m22}$ be the likelihood function, where $P_{ij} = P\{X_{t+1}=j \mid X_t=i\}$ and by equation (4), $P_{12} = 1-P_{11}$ and $P_{21} = 1-P_{22}$

Substituting for P_{12} and P_{21} in the above equation the likehood function becomes

$L(X_1, X_2, ..., X_m) = P_{11}^{m11} \times (1-P_{11})^{m12} \times P_{22}^{m22} (1-P_{22})^{m21}$

Taking the partial derivatives of the logarithm of the likelihood (the optimum of the logarithm of the likelihood function is achieved at the same location as the function itself) we have

$$\delta \ln L/\delta P_{11} = \delta/\delta P_{11}\{\ln(P_{11}^{m11} \times (1-P_{11})^{m12} \times P_{22}^{m22} (1-P_{22})^{m21})\}$$

$$= m11/P_{11} - m12/(1-P_{11}) = 0 \text{ for optimum value at } P_{11}$$

Similarly

$\delta \ln L/\delta P_{22} = m22/P_{22} - m21/(1-P_{22}) = 0$ for optimum value at P_{22}

Solving the system of these equations we have

$P_{11} = m11/(m11+m12) = m11/m1$

$P_{22} = m22/(m22+m21) = m22/m2$

$\delta^2/\delta P_{11}^2(\ln L()) = -m11/P_{11}^2 - m12/(1-P_{11})^2 < 0$ thus maximum at P_{11}

$\delta^2/\delta P_{22}^2 (\ln L()) = -m22/P_{22}^2 - m22/(1-P_{22})^2 < 0$ thus maximum at P_{22}

By generalization, the elements of the TMP are determined by n_{ij}/n_i, where n_{ij} is the number of transitions from state i to state j in one step and n_i is the number of times the process is in state i.

Appendix II: Euclidean distance and Centroid definitions

A. **Euclidean** is a standard mathematical measure of distance, **d(i,k)**,defined as follows:

$$\mathbf{d(i,k)} = [\Sigma(x_{ij} - x_{kj})^2]^{0.5}$$

Where d(i,j) in row i and column j is the distance between observations i and j.

B. The **Centroid** is the middle of a cluster. It is a vector containing one number for each variable, where each number is the mean of the variable for the observations in that cluster.

Appendix III: Listing of Example Programs

A. Program "ConvertState" transforms streamflow values into states of flow for Akitio winter calibration.

```
program ConvertState;
const
 MaxItems =1463;{Maximum number of observations}
type
  Flow = array[1..MaxItems] of real;
var
 x:Flow;
 InData, OutData1, OutData2:text;
 I:integer;
 sum1,sum2,sum3,sum4,sum5,sum6:real;
 a,b,c,d,e,f,j:integer;
begin
 Assign(Indata,'a:akwinter.cal');
 Assign(OutData1,'c:\fred\akwstate.cal');
 Assign(OutData2,'c:\fred\akwcount.cal');
 reset(InData);
 rewrite(OutData1);rewrite(Outdata2);
 a:=0;
 b:=0;
 c:=0;
 d:=0;
 e:=0;
 f:=0;
 sum1:=0;sum2:=0;sum3:=0;sum4:=0;
 sum5:=0;sum6:=0;
 for j:=1 to MaxItems do
```

```
begin
 read(Indata,x[j]);
 if((x[j]≥ 0) and (x[j]<3212)) then { streamflows in [0, 3212] in l/s}
   begin
    a:=a+1;
    sum1:=sum1+x[j];
    i:=1; {i is the state of flow}
   end
  else if((x[j]≥3212) and (x[j]<4262)) then
   begin
    b:=b+1;
    sum2:=sum2+x[j];
    i:=2;
   end
  else if((x[j]≥4262) and (x[j]<4762)) then
   begin
    c:=c+1;
    sum3:=sum3+x[j];
    i:=3;
   end
  else if((x[j]≥4762) and (x[j]<7480)) then
   begin
    d:=d+1;
    sum4:=sum4+x[j];
    i:=4;
   end
  else if((x[j]≥7480) and (x[j]<12227)) then
   begin
    e:=e+1;
    sum5:=sum5+x[j];
    i:=5;
```

```
      end
     else { Flood state interval}
      begin
       f:=f+1;
       sum6:=sum6+x[j];
       i:=6; {Flood state}
      end;
    writeln(OutData2,i:1);
  end;{for}
if a<>0 then
  writeln(OutData1,' R1 contains  ',a:1,' (',(sum1/a):1:2,')')
  {Output: state 1 contains "a" observations, mean flow "(sum1/a)"l/s}
else
 writeln(Outdata1,' R1 contains no observations.');
if b<>0 then
 writeln(OutData1,' R2 contains ', b:1,' (',(sum2/b):1:2,')')
else
 writeln(Outdata1,' R2 contains no observations.');
if c<>0 then
 writeln(OutData1,' R3 contains ', c:1,' (',(sum3/c):1:2,')')
else
 writeln(Outdata1,' R3 contains no observations.');
if d<>0 then
 writeln(OutData1,' R4 contains ', d:1,' (',(sum4/d):1:2,')')
else
 writeln(Outdata1,' R4 contains no observations.');
if e<>0 then
 writeln(OutData1,' R5 contains ', e:1,' (',(sum5/e):1:2,')')
else
 writeln(Outdata1,' R5 contains no observations.');
if f<>0 then
```

```
 writeln(OutData1,' R6 contains ', f:1,' (',(sum6/f):1:2,')')
else
 writeln(Outdata1,' R6 contains no observations.');
 close(OutData1);
 close(Outdata2)
end.
```

B. Program "Helpcount" counts state to state transitions

```
program HelpCount;
const
    MaxState = 6;
var
 j:integer;InData:text;
 outfile:text;
procedure Count (j:integer);
const
    MaxItems =1464;
type
 IndexRange=1..MaxItems;
 StateArray=array[IndexRange] of integer;
var
 InData:text;
 x:StateArray;
 i:IndexRange;
 a1,a2,a3,a4,a5,a6:integer;
begin { Count}
 Assign(Indata,'a:akwcount.dat');
Reset(Indata);
  a1:=0;a2:=0;a3:=0;a4:=0;a5:=0;
  a6:=0;
  i:=1;
  while i≤MaxItems do
    begin
      Read(Indata, x[i]);
      i:=i+1;
    end;
  for i:=1 to (MaxItems-1) do
   if(x[i]=j) then
```

```
      begin
       if(x[i+1]=1) then
        a1:=a1+1
        else if(x[i+1]=2) then
         a2:=a2+1
        else if(x[i+1]=3) then
         a3:=a3+1
        else if(x[i+1]=4) then
         a4:=a4+1
        else if(x[i+1]=5) then
         a5:=a5+1
        else
         a6:=a6+1
      end;
  writeln(outfile,a1:4,a2:4,a3:4,a4:4,a5:4,a6:4);
Close(Indata)
end;{Count}
begin{ HelpCount}
 assign(outfile,'a:akwfreq.dat'); rewrite(outfile);
 j:=1;
 while j≤MaxState do
  begin{while}
   Count(j);
   j:=j+1
  end;{while}
  close(outfile);
end.{ HelpCount}
```

C. Program "AssessThdfct" assesses the model perfomance forecasts by Threshold Forecasts approach.

```
program AssessThdfct;
const
   MaxState=6;
   MaxItems =732;{Maximun number events}
type
 ProbTable=array[1..MaxState,1..MaxState] of real;
 IndexRange=1..MaxItems;
 StateArray=array[IndexRange] of integer;
var
 InData, OutData,Inputfile,Outputfile:text;
 x:StateArray;
 i:IndexRange;
 j,p,q:integer;
 prob:ProbTable;
 a,b,c,d,xi,xiplus1:integer;
 maxval,p0:real;
begin { Assess}
 Assign(Inputfile,'a:akwcount.dat');
 Assign(Indata,'a:awpro.dat');
 Assign(OutData,'a:awresult.txt');
 Reset(Indata); rewrite(Outdata);
 Assign(Outputfile,'a:awftn.cal');rewrite(Outputfile);
 for i:= 1 to MaxState do begin
     for j:=1 to MaxState do
        begin
           read(Indata,prob[i,j]);
        end;
  end;
```

```
q:=Maxstate;p0:=0.0;
While p0 ≤1.01 do
 begin
  Reset(Inputfile);
  a:=0; b:=0; c:=0; d:=0;
  for i:=1 to maxitems-1 do begin
     Readln(Inputfile, xi,xiplus1);
     x[i]:=xi;
     x[i+1]:=xiplus1;
     p:=x[i];
     if(prob[p,q] ≥p0) then begin
       if(x[i+1]=MaxState) then
         a:=a+1  {nHf}
       else
         b:=b+1 {nFA}
      end else begin
        if(x[i+1]<>Maxstate) then
          c:=c+1  {nHnf}
        else
          d:=d+1;  {nMs}
      end;
   end;{for Maxitems-1}
writeln(Outdata,'At p0 ',p0:4:2,' nHf = ',a:4,' nM = ',d:4,'nFA = ',b:4,' nHnf = ',c:4);
 writeln(Outputfile,'At p0 ',p0:4:2,' P(FA) =',(b/(c+b)):5:4);
 writeln(Outputfile,'At p0 ',p0:4:2,' P(Mis)=',(d/(a+d)):5:4);
 p0:=p0+0.01;
 end;{while}
close(Indata);
close(outdata);
close(Outputfile);
end.
```

D. Program "MPEvent" assesses the model performance by the Most approach:

```
Probable Event forecasts.
program MPEvent;
const
   MaxState=6;
   MaxItems =121;
type
 ProbTable=array[1..MaxState,1..MaxState] of real;
 State=array[1..MaxItems] of integer;
 maxprobTable=array[1..Maxstate] of real;
var
 Probdata, Statedata,maxprodata,fctdata,transit:text;
 x:State;
 prob:ProbTable;
 maxprob:maxprobTable;
 i,p,q,fctstate,l:integer;
 maxval,u,v:real;
begin {MPEvent}
 Assign(probdata,'a:aspro.dat');
 Assign(statedata,'a:akscount.ve1');
 Assign(maxprodata,'a:asmaxpro.dat');
 Reset(probdata);
 Reset(statedata);
 Rewrite(maxprodata);
 Assign(fctdata,'a:mpedata.out');
 Rewrite(fctdata);
 for p:= 1 to MaxState do
  begin
   maxval:=0;
     for q:=1 to MaxState do
```

```
      begin
        read(probdata,prob[p,q]);
        if prob[p,q]>maxval then maxval:=prob[p,q];
      end;
      writeln(maxprodata,maxval:1:5);
end;
close(probdata);
close(maxprodata);
reset(probdata); Reset(maxprodata);
for p:=1 to maxstate do
 begin
  read(maxprodata,maxprob[p])
 end;
for i:=1 to MaxItems do
 begin
  read(statedata,x[i]);
  p:=x[i];
  u:=maxprob[p];
  for q:=1 to MaxState do
   begin
   l:=i+1;
    v:=prob[p,q];writeln(fctdata,l,' ',p,' ',q,' ',u:1:5,' ',v:1:5);
   end;
 end;
close(probdata);
close(maxprodata);
close(fctdata);
reset(fctdata);
assign(transit,'a:asmpever.dat');
rewrite(transit);
while not EOF(fctdata) do
```

```
 begin
  while not EOLN(fctdata) do
   begin
    readln(fctdata,l,p,q,u,v);
    if(abs(u-v)<0.0000001) then
     begin
      writeln(transit,l,' ',x[i+1],' ',q);
     end;
   end;
 end;
close(statedata);
close(transit)
end.
```

Appendix IV: MPE Summer Objective function values.

Table A1: MPE Multi-objective function points. Akitio River, summer calibration.

p_0 /(Point)	P(FA)	P(Ms)
0.00 - 0.449 (f)	1.0000	0.0000
0.45 - 0.559 (e)	0.9648	0.0714
0.56 - 0.629 (d)	0.9550	0.4286
0.63 - 0.829 (c)	0.9226	0.6429
0.83 - 0.949 (b)	0.6526	0.8571
0.95 - 1.000 (a)	0.0000	1.0000

Table A2 MPE Multi-objective function points. Akitio River, summer verification.

p_0 /(Point)	P(FA)	P(Ms)
0.00 - 0.449 (f)	1.0000	0.0000
0.45 - 0.559 (e)	0.9316	0.0000
0.56 - 0.629 (d)	0.9231	0.6667
0.63 - 0.829 (c)	0.8632	1.0000
0.83 - 0.949 (b)	0.3932	1.0000
0.95 - 1.000 (a)	0.0000	1.0000

Table A3 MPE Multi-objective function points. Makakahi River, summer calibration.

p_0 /(Point)	P(FA)	P(Ms)
0.00 - 0.389 (g)	1.0000	0.0000
0.39 - 0.449 (f)	0.9753	0.0000
0.45 - 0.529 (e)	0.9564	0.4375
0.53 - 0.619 (d)	0.8880	0.6250
0.62 - 0.629 (c)	0.7173	0.8125
0.63 - 0.929 (b)	0.6888	0.8750
0.93 - 1.000 (a)	0.0000	1.0000

Table A4 MPE Multi-objective function points. Makakahi River, summer verification.

p_0 /(Point)	P(FA)	P(Ms)
0.00 - 0.389 (g)	1.0000	0.0000
0.39 - 0.449 (f)	0.9744	0.0000
0.45 - 0.529 (e)	0.9316	0.6667
0.53 - 0.619 (d)	0.8889	0.6667
0.62 - 0.629 (c)	0.6581	1.0000
0.63 - 0.929 (b)	0.6068	1.0000
0.93 - 1.000 (a)	0.0000	1.0000

For the Kiwitea Stream does not seem to have floods during summer months, thus no model application was made.

Appendix V

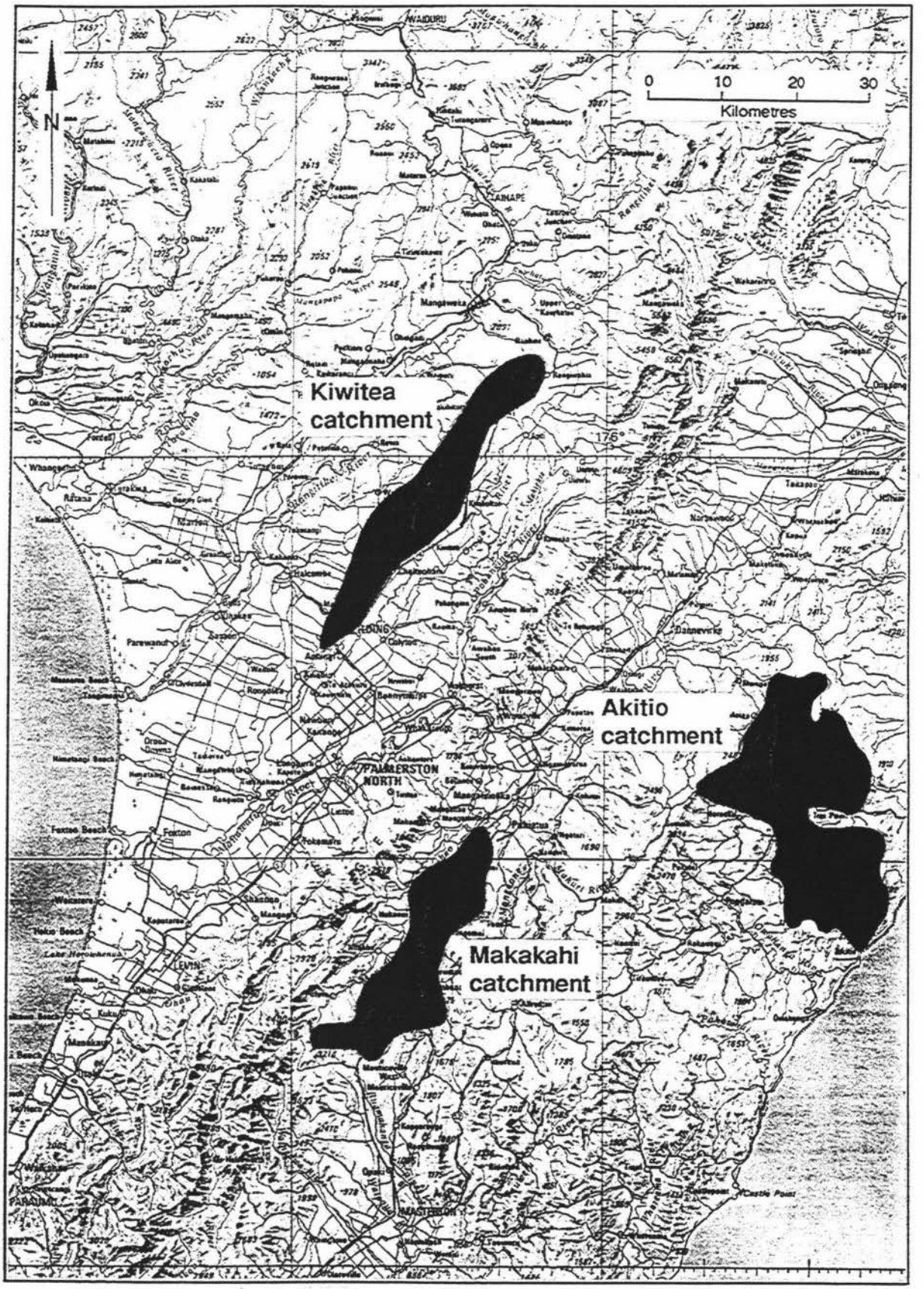

Fig. A.1 The Akitio, Makakahi and Kiwitea catchments